**Title**
The prediction of human cortical bone strength using the finite element method



**Author**
Rossi, Stephen Andrew

**Publication Date**
1996

Peer reviewed|Thesis/dissertation

# THE PREDICTION OF HUMAN CORTICAL BONE STRENGTH USING THE FINITE ELEMENT METHOD:

## A STUDY OF THE FLEXURAL AND TORSIONAL BEHAVIOR OF FEMORAL SHAFTS WITH SIMULATED METASTATIC LESIONS

by

**STEPHEN ANDREW ROSSI**

DISSERTATION

Submitted in partial satisfaction of the requirements for the degree of

DOCTOR OF PHILOSOPHY

in

**BIOENGINEERING**

in the

GRADUATE DIVISIONS

of the

UNIVERSITY OF CALIFORNIA SAN FRANCISCO

and

UNIVERSITY OF CALIFORNIA BERKELEY

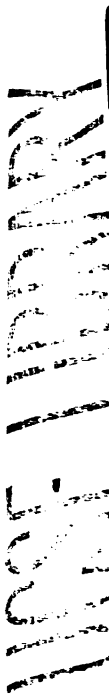

*This work is dedicated to my father, William Rossi, Jr.,*
*a man whose complete fascination by science and unfailing faith in me*
*have always encouraged my pursuit of knowledge.*

# Acknowledgments

In the twenty-eight years of my being, this will be my first written acknowledgment. I hope that I have not waited until this point, the completion of my doctoral dissertation, to thank those who have enriched and enlightened me throughout the years. If I have indeed failed to acknowledge those outstanding individuals in the past, then these pages are chance to finally rectify such an omission. I would like to believe I have already thanked the important participants in my academic and personal development with both words and deeds. These pages would then serve to remind me of how lucky I am to have had such support.

First I must acknowledge those most directly responsible for the completion of my dissertation and the conferment of my degree. Harry Skinner, Doctor of both Philosophy and Medicine, was the man who took in that naive student five years ago. With an ability to inspire performance without commanding it, Dr. Skinner allowed me to create my own path. Few students have had the opportunity to write a grant proposal, define an entire project, and conduct independent research as I have. It was his faith in my ability to do good science that fostered my independence and spurred my growth. Dr. Steve Lehman boasted an important role in my academic progression, whether as graduate student advisor, chair of my qualifying examination committee, or member of my thesis committee. By treating me as an equal regardless of whether I had earned that status, he became an important sounding board for my making important decisions. I respect Steve a great deal for his complete dedication to both the advancement of science and the achievement of young scholars. I need to thank two other professors for their participation on my quals and thesis

committees: Dr. James Johnston and Dr. Jeff Lotz. These professors dissected my ideas with a critical eye, contributing their expertise to the performance of sound research.

If grad school were likened to war, it was Joyce Keyak with whom I fought in the trenches. It was her bullet-sharp mind and vigilant guard that saved me from many of the pitfalls of the research experience. For much of the Six Year's War, it was only she with whom I could share my ideas. Many other soldiers came and went (Rob Fassberg, Kim Jones, Irving Lee, and Louis Vu), helping with both little details and the big ideas. Without their assistance, the war would still be raging on. If graduate school were likened to family, Debra would be the mother to all of us bioengineering students. Her keen mind and compassionate heart were our only defense against administrative quagmires and personal nightmares. As students, we were brothers and sisters in the travails toward candidacy and beyond. There are a few students in particular that buttressed me in my efforts toward academic success: Kevin Clark, Kathy Cortopassi, Margot Damaser, Sue Moyher, Liz Penades, Peter Quesada, and Mary Wagner. In our sharing common graduate experiences, we were able to constructively vent our frustrations and share our successes.

But graduate school is neither a war nor a family; it is just long hard work. That is why the technical support of Frank Ashford and Moira Heilmann became invaluable. That is why the administrative support of Elizabeth Jameson proved essential. That is why the craftsmanship of Laszlo Bosckai and William Doyle seemed indispensable. Of course in addition to contributing their talent, they contributed their generosity and warmth, two qualities often lacking in people within a research institution. I will also use this opportunity to thank the hands that fed me: Department of Veterans Affairs, Rehabilitation Research and Development Service for their generous funding of my research; the UCSF

Anatomy Department, UCSF Tissue Bank, Central California Blood Bank Tissue Service, and National Disease Research Interchange for their provision of human specimens; and California Advanced Imaging for the use of their CT scanning capabilities.

Outside the realm of the academic world is the real world – the world where many significant others have contributed their thoughtfulness to making my life rich and whole. First and foremost, I owe much to the people who brought me into this world, William and Dorothy Rossi. As parents and role models, they were tireless in their dedication to raising children with curious minds and compassionate hearts. I have also valued the support of my brothers and sisters in the Rossi Clan (Mike, Traci, Jeff, Cynthia, and Matt). Beyond my God given family were the kindred spirits that I have chosen as family. It would be impossible to describe the importance of each of these individuals, but let a simple list serve to honor them.

Faith Bertrand

Steve Raiff • Kathleen Gerety

Catherine Hopman • Michael Cuesta • Kim Ranalli

David Quigg • Denise Shushan

Chris Covin

I hope that I have indeed accomplished what I set out to accomplish – to thank those whom I have forgotten to thank and to remind myself of my own good fortune.

# Abstract

Current methods for determining the risk of fracture for bones with metastatic lesions are inadequate. This research investigated the flexural and torsional behavior of femoral shafts with simulated lesions as a means toward improving clinical guidelines. Four-point bending tests demonstrated differences in the failure characteristics of whole bones and bones with hemispherical defects; whole bones exhibited greater structural ductility with five times the energy-to-failure ($p < 0.01$). Linear finite element (FE) models predicted failure loads for both sets of bones *a priori* and demonstrated the benefit of using computed tomography (CT) scan data to describe bone geometry and density-based heterogeneity. Models not utilizing CT scan data were less accurate and precise ($r = 0.76$) than models using CT scan data for geometry ($r = 0.93$) or for both geometry and heterogeneous material properties ($r = 0.97$). A parametric sensitivity analysis revealed that linear FE models could not explain the differences in structural behavior of whole bones and bones with defects. Nonlinear models that incorporated a bi-linear stress-strain relationship for cortical bone performed as well as linear models in predicting ultimate strengths for the flexural experiment ($r = 0.99$). Moreover, the behavior of these nonlinear models provided a possible explanation for differences in ductility between the two sets of bones; perhaps, the "brittle" failure of bones with defects was the consequence of early but concentrated plastic yielding, imperceptible on macroscopic load-deflection curves. CT scan-derived linear models were then used to predict the torsional strengths of bones with hemispherical defects. The linear FE models achieved high precision ($r = 0.99$), but overestimated ultimate torques by a factor of two. This was most likely the consequence of a failure

criterion that did not account for the orthotropy of cortical bone. Future studies should address the issue of material property assumptions and failure criteria used in the modeling of cortical bone structures. Until that time, the precision of the CT scan-derived FE models of this investigation marks a significant step toward the prediction of failure for bones with metastatic lesions.

## Dissertation Committee Members

Harry Skinner, M.D., Ph.D. (Chair)

James Johnston, M.D.

Steven Lehman, Ph.D.

Jeff Lotz, Ph.D.

# Table of Contents

# Tables

# Figures

# Chapter I

## Introduction and motivation

With the aging United States population, the overall cancer death rate has been increasing at the rate of 0.4% per year (Stephens, 1991). It has become the second leading cause of death, accounting for 24% of all deaths in 1984 (Harrington, 1988). The increased incidence of cancer brings an attendant increase in the incidence of metastatic lesions found in bones, the common causes being cancers of the breast, kidney, lung, and prostate. It is estimated that as many as 90% of patients dying of disseminated malignancy have bone metastases (Rubens and Fogelman, 1991). Though only 10% of patients with bone metastases actually sustain pathological fracture, the consequences of fracture are so devastating that prophylactic management of individual lesions becomes essential. With a 5 year survival rate of 60%, breast cancer has a particularly long survival time following the development of bone metastases (Myers and Ries, 1989), and accounts for 60% of all pathological fractures (Harrington, 1988). Because the most common site of fracture secondary to breast cancer is the femur, a bone of great functional importance, the orthopaedic management of metastatic carcinoma in the femur requires significant attention.

Metastatic carcinoma usually has devastating consequences on the patient; however, aggressive palliative treatments including a sophisticated combination of hormone manipulation, chemotherapy, and radiation therapy

have been successful in prolonging life. With prolonged life comes the concomitant increase in the presence of bone metastases and subsequent bone fractures. Treatment of metastatic lesions of the bone often includes radiation therapy, which can effectively halt the progression or even stimulate the regression of a lesion (Harrington, 1982). Moreover, radiation therapy provides the most effective means of relieving bone pain. Unfortunately, radiation therapy and the subsequent osteonecrosis can lead directly to pathological fracture. For cases in which fracture occurs, stabilization of the fracture is required in order to ease the pain, improve patient care, and offer the only opportunity for the restoration of ambulatory skills (Murray and Parrish, 1974). Treatment by bed rest is a poor solution, as fracture healing is rare in irradiated bone, and many complications result from extended immobilization. With the advent of methylmethacrylate as an augmentation to fixation, successful fixation has become more common and patient survival rates have improved (Habermann et al., 1982).

A major goal in the management of skeletal metastases is sparing patients the trauma of pathological fracture. One strong argument for prophylactic fixation of impending fractures is that post-operative survival rates for those undergoing prophylactic fixation is significantly higher than for those undergoing fracture fixation for pathological fracture (Hardman et al., 1992). Additional evidence suggests irradiated bone can heal provided internal fixation is used to avoid fracture (Bonarigo and Rubin, 1967). Averting pathological fracture also yields the obvious benefits of allowing early ambulation, decreasing hospital stay, reducing operative difficulty, and reducing pain when compared with the treatment of pathological fracture. The issue then becomes the evaluation of metastatic defects to determine fracture risk. Currently, the criteria for determining the need for providing prophylactic fixation

are based on empirical evidence and consist of the following: (1) femoral bone destruction exceeding 50% of the cortex; (2) lesions larger than 2.5 cm in diameter in the proximal femur; (3) lesions involving the lesser trochanter; and (4) persistent pain despite irradiation. These criteria are rough guidelines based on radiographic evidence and leave much to the discretion of the surgeon.

The shape and characteristics of metastatic lesions in bone vary depending on the type of tumor and the rate of tumor progression. The appearance of a lesion is usually described with the terms *geographic*, *moth-eaten*, or *permeative*, depending on whether its effects are localized, distributed, or diffuse, respectively. In general, faster growing tumors are more permeative in nature and do not have sharply marginated borders. Unless a lesion is geographic in nature, the involvement of cortical bone is difficult to assess from plane radiographs. Even geographic lesions must be larger than 1.5 cm and demonstrate 50% loss of bone mineral content before they are detectable by x-ray (Rubens and Fogelman, 1991). The use of computed tomography (CT) scans can assist in early tumor detection and in evaluation of metastatic lesions, benefiting from higher resolution, sharper contrast, and three dimensional capabilities. It seems likely that improvement in the criteria for determining lesions at high risk of fracture would come from the implementation of this more advanced technology.

The research described in the following manuscript has been performed within the context of developing improved criteria for determining the risk of fracture for bones containing metastatic lesions. Clinical practice currently uses defect size as the determinant of fracture risk, which assumes that risk of fracture is a function of bone strength. Accepting this premise, the present study targeted predicting the strength of bones *in vitro* as a means toward the ultimate

goal of improved clinical guidelines. Because of limitations in using two-dimensional radiographic evidence for evaluating bone strength, this study used CT scan data as a tool for assessing the three-dimensional geometry and density variation in human femoral shafts. These data were incorporated into three-dimensional finite element (FE) models for the evaluation of stresses and prediction of failure loads. Strengths predicted by the FE models were then compared with the results of flexural and torsional mechanical testing. By validating FE models for failure prediction and the dissecting basic modeling assumptions, the present study examined the following hypotheses: (1) using CT scan data to characterize geometry and material properties increases FE model precision; (2) including the simplifying assumptions of material homogeneity, elasticity, isotropy, and symmetry limit FE model generality and accuracy. More specific objectives are detailed below.

- To compare the flexural load-deflection characteristics of whole bones to those of bones with hemispherical defects.
- To show that using CT scan data to describe geometry and material heterogeneity increases the precision of FE flexural strength predictions.
- To explore the modeling of cortical bone plasticity as a means of explaining cortical bone structural behavior.
- To validate linear CT scan-derived FE models for predicting torsional failure loads of bones with hemispherical defects.
- To evaluate the influences of geometry and material properties on the structural behavior of cortical bone using established engineering theory.

# Chapter II

## Strength of bones with defects

Prophylactic fixation of an impending fracture is always preferable to the treatment of pathological fracture. Predicting the likelihood of fracture, however, poses a challenging question that requires, in part, an understanding of how bone responds mechanically to the presence of a defect. For this reason, some investigators have performed retrospective studies of patients with metastatic lesions in order to ascertain the risk of fracture based on tumor geometry and location. Others have approached the question from a more fundamental perspective by addressing the issue of the actual strength of bones with experimentally-introduced defects. The premise of such studies is that a better appreciation of strength reductions caused by metastatic lesions will lead to a clinical tool for evaluating fracture risk.

### *Radiographic studies*

The current clinical criteria are derived from early investigations into using the radiographic assessment of metastatic defects for determining fracture risk. A retrospective study of 118 metastatic breast cancer patients found that 58% of the bones that fractured met a 2.5 cm criteria, and used that information to imply that the 2.5 cm criteria was predictive over 50% of the time (Beals et al., 1971).

Since they did not report on the percentage of defects meeting the criteria that did not fail, it is difficult to determine if this criterion was truly predictive. A subsequent study evaluated the radiographs of 66 consecutive patients and categorized defects into four groups by percentage of cortical involvement (Fidler, 1981). Fidler found marked increases in the failure rate when defects exceeded 50% cortical involvement. Other retrospective studies have concluded that the presence of pain foretells pathologic fracture and calls for surgical fixation (Schurman and Amstutz, 1973).

Keene et al. evaluated the use of radiographic criteria for judging the need for prophylactic fixation by studying skeletal metastases from carcinoma of the breast, the form of tumor responsible for 30% to 50% of long bone fractures (Keene et al., 1986). This study of 2,673 breast cancer patients found no statistically significant difference in the percentage of cortical involvement for bones that failed and those that did not. It was explained that the variability in radiograph depictions of tumors made them of little predictive value; the same tumor could appear completely different in size depending on radiographic orientation. Additionally, the majority of tumors witnessed were a permeative type that were not amenable to measurement. The authors concluded that radiographic criteria were unacceptable and that future studies should look to the use of CT scan data.

## *Experimental studies*

The previous studies were aimed at developing radiographic criteria, but the limited nature of radiographic measurements confounded their ability to derive definitive criteria. Several investigators turned to experimental studies to begin

to explore the mechanical strength of bones and changes in strength with the presence of defects. By loading bones in torsion, Brooks et al. showed that 2.8 and 3.6 mm drill holes in canine femora reduced the energy absorbing capacity by 55% (Brooks et al., 1970). The calculated stress concentration factors associated with these load reductions were considerably less than those expected from an elastic homogeneous isotropic material, which was attributed to the natural presence of defects and inhomogeneities in bone. Clark et al. found that the torsional strength of human femora was more dependent on the width of the defect than on its length (Clark et al., 1977). A study by Leggon et al. found that bones with defects involving 50% of the cortex retained only 12.7% of the intact torsional strength and recommended both plating and cementing the bone (Leggon et al., 1988). Though not suggesting new criteria for identifying metastatic bones at risk of fracture, these studies demonstrated significant factors affecting bone strength that the 50% rule of thumb had not recognized.

Edgerton et al. studied the effect of defect size on bone strength by testing sheep femora in torsion with defect sizes ranging from 10% to 60% of the bone diameter (Edgerton et al., 1990). This study found no statistically significant reduction in strength until defects exceeded 10% of the bone diameter, consistent with the presence of natural defects and inhomogeneities in bone. With 20% defects, bone strength had dropped dramatically but followed a more gradual, linear decrease until reaching 28% of its original ultimate torque at a defect size of 60%. This study suggested that a more prudent criterion for fracture fixation would consider defects 33% of the bone diameter, the value at which bone strength was approximately halved. However, this new criterion arbitrarily set the threshold and did not address the issue of problematic radiographic assessment of tumor size.

## *Finite element modeling studies*

McBroom et al. conducted the first study to model trends in the strength reduction of bones with increasing defect size (McBroom et al., 1988). In this study, drilled holes served as defects in canine femora which were then subjected to four-point bending. Simplified cylindrical finite element models provided the stress distributions needed to correlate the experimental failure stresses with theoretical predictions. The authors found linear FE models predicted the correct stress concentrations according to engineering literature, but that elastic-plastic finite element models better predicted the decrease in bone strength exhibited by the experiment. This study was valuable in showing that the traditional criterion, which uses 50% of the cortical diameter as the critical parameter, does not account for severe weakening caused by defects smaller than 50% of the bone diameter. Shortcomings of this study included its use of simplified geometry, canine femora, and non-biological loading conditions. For clinical relevance, the study recommended the use of CT scan data to model the rough cortical boundaries of metastatic defects.

Hipp et al. continued the search for appropriate criteria with a study on the structural consequences of endosteal lesions (Hipp et al., 1989). Canine femora were reamed to simulate endosteal defects, and then subjected to four-point bending. CT scans were used to approximate the geometry needed for both a bending and torsional FE model of each bone tested. In contrast with the previous study, this study found that both a linear and elastic-plastic model correlated with the experimental results, which can be explained by the absence of the sharp stress risers previously caused by drill holes. Interestingly, the site of minimum cortical thickness, a location which can only

be determined from CT scan data, was the point of maximum stress and the most significant geometric parameter for predicting failure. Additionally, the models demonstrated a sensitivity to the reduction of material properties at the margins of defects, suggesting the importance of characterizing partially demineralized bone found near metastatic lesions *in vivo*. A limitation of this study was the dependence on artificial geometry, not only in modeling but also in the normalization of experimental data to determine strength reductions. This study also emphasized the need for CT scan data to obtain more accurate geometric information.

Finite element modeling of long bones in torsion was conducted by Hipp et al. (Hipp et al., 1990) in an effort to explain the strength reduction data generated by sheep experiments (Edgerton et al., 1990). A linear model underestimated the strengths found in the experimental results, while an elastic-plastic model overestimated the strengths. Neither model explained the shape of the strength retention curves found by the torsional experiment. The authors implied that the conservative predictions of strength by linear modeling would be more appropriate for developing clinical fracture risk criteria. Once again, cortical wall thickness seemed to be an important factor in predicting strength. The poor correlations achieved by this study were attributed to deficiencies in mesh density, boundary conditions, failure criterion, material properties, and geometry. Two valuable insights came from this study: (1) linear models can provide reasonable correlations with experimental results and are far less computationally demanding; and (2) the decreasing elastic modulus in the region of a metastatic tumor should be incorporated into the model, for it not only affects torsional stiffness but also reduces stress concentrating effects.

A recent study by Kuo et al. criticized previous works for not identifying the true location of maximum stress relative to the defect (Kuo et al., 1991). By

testing acrylic rods in torsion, this study found a shift in the maximum stress with increasing defect size and maintained that stress distributions were highly dependent on local geometry. According to Kuo et al., these findings suggest that strength reduction characteristics in the long bones of one species may not be applicable to another. The study added that future studies should concentrate on geometric irregularity.

Cheal et al. performed the most sophisticated finite element modeling of human femurs with metastatic defects (Cheal et al., 1993). With seventeen matched pairs of proximal femurs, they hoped to demonstrate the strengths associated with superior-lateral and inferior-medial defects in the femoral neck. The authors used a 550 element representative model containing both cortical and trabecular elements to identify the failure strengths caused by an axial load through the femoral head. Unfortunately, the model underestimated strengths by a factor of three and failed to quantify the difference between inferior-medial and superior-lateral defects. The authors attributed the study's poor correlations to two facts: (1) the model femur was not representative of the population; and (2) the model did not account for material property variation.

The literature cited above details the scientific events leading up to my decision to pursue improved methods for determining the strength of human cortical bones with simulated metastatic lesions. Many issues confounded the ability of these studies to successfully predict failure. Recurrent problems included the use of simplified geometry, non-representative models, non-human femurs, insufficient mesh densities, and homogeneous material properties. Equal import was given to the need for future studies to investigate the use of CT scan data, especially for cases of irregular geometry and heterogeneous material properties. The present study strove to address these issues in the development of new modeling techniques to predict femoral

fracture. By using CT scan data to develop three-dimensional FE models, this research benefited from the following: (1) use of human bone specimens; (2) rapid generation of FE models with small elements; (3) accurate assessment of bone and defect geometry; and (4) heterogeneous material properties based on bone densitometry.

# Chapter III

## Mechanical properties of bone tissue

Before establishing a methodology for studying femoral bone strength, it was important to examine current knowledge of cortical bone biomechanics. Many researchers have studied cortical bone in an attempt to link its biology with fundamental mechanics. It is from this research that the basic modeling assumptions for the present study were derived.

### *Materials testing*

Human cortical bone is a fibrous organic matrix whose major constituents are hydroxyapatite crystals (45%), bone collagen (35%), and water (20%). Cortical bone varies in porosity from about 5% to 30% and has an approximate apparent density of 1.8 g/cc, where apparent density is defined as tissue mass divided by bulk volume (Carter and Spengler, 1978). While the composition of cortical bone is relatively uniform, its structure can vary depending on whether it is primary or secondary bone. Primary bone is that bone formed directly by endochondral ossification or subperiosteal deposition and is dominantly lamellar in human long bones. It can be found in the form of circumferential lamellae, which line the periosteal and endosteal surfaces of the bone, or in the form of primary osteons, which are characterized by tight concentric lamellae

without any cement lines. However, the majority of adult cortical bone is secondary bone, the product of extensive remodeling through osteoclastic and osteoblastic activity (Ross et al., 1989). The resultant Haversian systems are concentric lamellae, 200 to 300 μm in diameter, that surround vascular channels and are bordered by cement lines (Martin and Burr, 1989). The purpose in understanding the organization of cortical bone is that its longitudinal arrangement and inherent porosity have natural consequences on mechanical properties.

| Direction | Testing Mode | Strength (MPa) |
|---|---|---|
| Longitudinal | Tension | 133 |
| | Compression | 193 |
| Transverse | Tension | 51 |
| | Compression | 133 |
| | Shear | 68 |

(Reilly and Burstein, 1975)

**Table 3.1** Ultimate strength properties of human femoral cortical bone

Reilly and Burstein conducted a particularly complete investigation into the mechanical properties of cortical bone (Reilly and Burstein, 1975). By testing both bovine and human bone in tension, compression, and torsion, this study derived transversely isotropic mechanical properties for cortical bone (**Table 3.1**). This study was followed by the work of Van Buskirk et al. in which the transverse properties were divided between the circumferential and radial directions (Van Buskirk et al., 1981). For the purposes of modeling bone as a structural material, it became customary to utilize the material properties derived

from these two studies, i.e. ultimate strengths, Young's moduli, Poisson's ratios, and shear moduli (**Tables 3.1** and **3.2**).

| Material Properties | Reilly & Burstein, 1975 | Van Buskirk et al., 1981 |
|---|---|---|
| $E_1$ (GPa) | 11.5 | 13.0 |
| $E_2$ (GPa) | 11.5 | 14.4 |
| $E_3$ (GPa) | 17.0 | 21.5 |
| $G_{12}$ (GPa) | 3.6 | 4.74 |
| $G_{13}$ (GPa) | 3.28 | 5.85 |
| $G_{23}$ (GPa) | 3.28 | 6.56 |
| $\nu_{12}$ | 0.58 | 0.37 |
| $\nu_{13}$ | 0.31 | 0.24 |
| $\nu_{23}$ | 0.31 | 0.22 |
| $\nu_{21}$ | 0.58 | 0.42 |
| $\nu_{31}$ | 0.46 | 0.40 |
| $\nu_{32}$ | 0.46 | 0.33 |

**Table 3.2** Elastic properties of human cortical bone

(Terms defined in **Equation 3.1**)

The stress and strain at a particular point within a material can be expressed as second-order tensors, mathematical representations that are independent of the particular Cartesian bases used to express their components (Cowin, 1989). The tensors of stress and strain can be related through a fourth-order material compliance tensor according to Hooke's Law (**Equation 3.1**). The material compliance matrix for an orthotropic material shows that strains arise from

normal and shear stresses with no coupling between the two, provided that the material is stressed along the principal material directions. For cortical bone, the coordinate system corresponding to the directional material properties has $x_1$ as the radial coordinate axis, $x_2$ as the circumferential coordinate axis, and $x_3$ as the longitudinal coordinate axis. The lack of coupling between shear and normal stresses holds only for directions coincident with the coordinate axes. The anisotropic qualities of cortical bone are important to mention, for they become a confounding variable in one's ability to predict bone mechanical behavior in nontrivial loading configurations.

$$[S_{ij}] = \begin{bmatrix} \frac{1}{E_1} & -\frac{\nu_{21}}{E_2} & -\frac{\nu_{31}}{E_3} & 0 & 0 & 0 \\ -\frac{\nu_{12}}{E_1} & \frac{1}{E_2} & -\frac{\nu_{32}}{E_3} & 0 & 0 & 0 \\ -\frac{\nu_{13}}{E_1} & -\frac{\nu_{23}}{E_2} & \frac{1}{E_3} & 0 & 0 & 0 \\ 0 & 0 & 0 & \frac{1}{G_{23}} & 0 & 0 \\ 0 & 0 & 0 & 0 & \frac{1}{G_{31}} & 0 \\ 0 & 0 & 0 & 0 & 0 & \frac{1}{G_{12}} \end{bmatrix}$$

| | | |
|---|---|---|
| $[S_{ij}]$ | = | Compliance coefficients |
| $E_i$ | = | Young's modulus in the i-direction |
| $\nu_{ij}$ | = | Poisson's ratio for strain in the j-direction when stressed in the i direction |
| $G_{ij}$ | = | Shear modulus in the i-j plane |

**Equation 3.1** Orthotropic elastic compliance tensor

Material strengths published in the literature are usually derived from uniaxial material tests. However, most loading configurations produce multiaxial stress states, requiring a more comprehensive method for relating a triaxial stress state to the results of a uniaxial test. The von Mises – or effective stress – criterion is the engineering approach used for most isotropic ductile metals (**Equation 3.2**). This failure theory postulates that yielding is due to the angular distortion of an element and is independent of hydrostatic stresses. The von Mises equation defines a yield surface for all triaxial stress states and requires only the result of a uniaxial tension or compression test. The complicating issue for cortical bone is that it does not behave isotropically; the strength of bone is highly dependent on loading direction as indicated above. Determining failure for orthotropic materials requires a more complicated failure criterion – such as the Tsa-Wu theory of failure (Tsai and Wu, 1971) – that would account for strength asymmetry and anisotropy. Cezayirlioglu et al. found good agreement between experiment and multiaxial failure theory for cortical bone (Cezayirlioglu et al., 1985) by using the equations of Tsai-Wu to determine failure for a variety of combined axial-shear loading conditions.

$$\sigma_{vonMises} = \frac{1}{\sqrt{2}}\sqrt{(\sigma_1-\sigma_2)^2+(\sigma_1-\sigma_3)^2+(\sigma_3-\sigma_2)^2}$$

| | | |
|---|---|---|
| $\sigma_i$ | = | Principal stress in the i-direction |
| $\sigma_{vonMises}$ | = | Effective stress |

**Equation 3.2** Von Mises failure criterion

The basic assumption of the preliminary reports on cortical bone material properties was material homogeneity. This assumption was subsequently challenged, and new theories began to arise about the variation of material properties in bone. By combining the results from compression tests on trabecular and cortical bone, Carter and Hayes found that compressive strength was proportional to the square of apparent density, and modulus proportional to the cube of density (Carter and Hayes, 1977). This study also found that modulus was slightly strain rate-dependent. Though this preliminary study had obvious limitations due to its use of bovine bone and insufficient cortical bone sampling, it was one of the first to examine the heterogeneity of bone material properties.

Cortical bone exhibits definite age-dependent characteristics. With age, there is progressive remodeling of cortical bone, resulting in an increased number of osteons and increased porosity (Martin, 1993). These structural changes correspond with a gradual deterioration of mechanical properties. McCalden et al. found that ultimate tensile strength and ultimate strain decreased dramatically with age; diminished post-yield behavior explained the majority of this decrease (McCalden et al., 1993). This study also found that all of the variation in strength could be explained by porosity alone and that mineral content and changes in microstructure had virtually no independent effects. This implied that material property information could be obtained from a knowledge of apparent density, an indirect measure of porosity.

Many studies have attempted to define cortical bone mechanical properties as functions of apparent density, with varying degrees of success. A complicating factor has been the narrow range of densities found in cortical bone; any experimental variability confounded the ability to derive accurate relationships. Schaffler and Burr found that the modulus of steer cortical bone

varied with apparent density raised to the power of 7.4 (Schaffler and Burr, 1988), higher than the power of 3 found by Carter and Hayes (Carter and Hayes, 1977). In a subsequent study, Keller et al. used four-point bending to test 155 specimens of human femoral diaphyseal bone with an apparent density range of 0.5 to 2.1 g/cc (Keller et al., 1990). The power associated the elastic modulus correlation was 1.54, and the power associated with the strength correlation was 2.18, with reported standard error of the mean (SEM) values of 0.07 and 0.09, respectively. A follow-up study by Keller tested 550 specimens of vertebral and femoral compact bone in compression and found that over 93% of the variation in modulus and strength could be explained by power functions of apparent density (Keller, 1994). He postulated that variations in the exponents found by different studies were largely a function of the range of data spanned; small ranges of higher density cortical bone would lead to higher power relationships. This strongly suggested that relationships found for a limited range of data, such as that for trabecular bone, cannot be extrapolated to include the entire data range. Lotz et al. investigated the three-point bending strength and stiffness of thin specimens of cortical shell and derived linear relationships between apparent density and mechanical properties (Lotz et al., 1991). Once again, mechanical property differences between proximal and distal bone were explained by density differences.

The key to understanding the power relationships found by the different studies is recognizing what data they represent. By graphing the findings of multiple studies on the same axes, it becomes clearer that the different relationships all represent pieces of some fundamental relationship that exists between density and mechanical properties (**Figures 3.1** and **3.2**). The differences in the magnitudes of the mechanical properties can be explained by experimental differences, i.e. loading modality, specimen origin, specimen

dimensions, and measurement techniques. For example, the extremely low magnitudes for modulus presented by Keller et al. can be attributed to the fact that flexural tests do not measure material properties directly and have errors associated with imprecise measurement of deformation (Keller et al., 1990). Despite discrepancies in the relationships found in the various studies, the consistency of the trends warrants the use of second-power relationships (Chapter IV) in the present study (**Figures 3.1** and **3.2**). Though only an approximation of the published data, these second-power relationships may account for some of the variability associated with cortical bone heterogeneity.

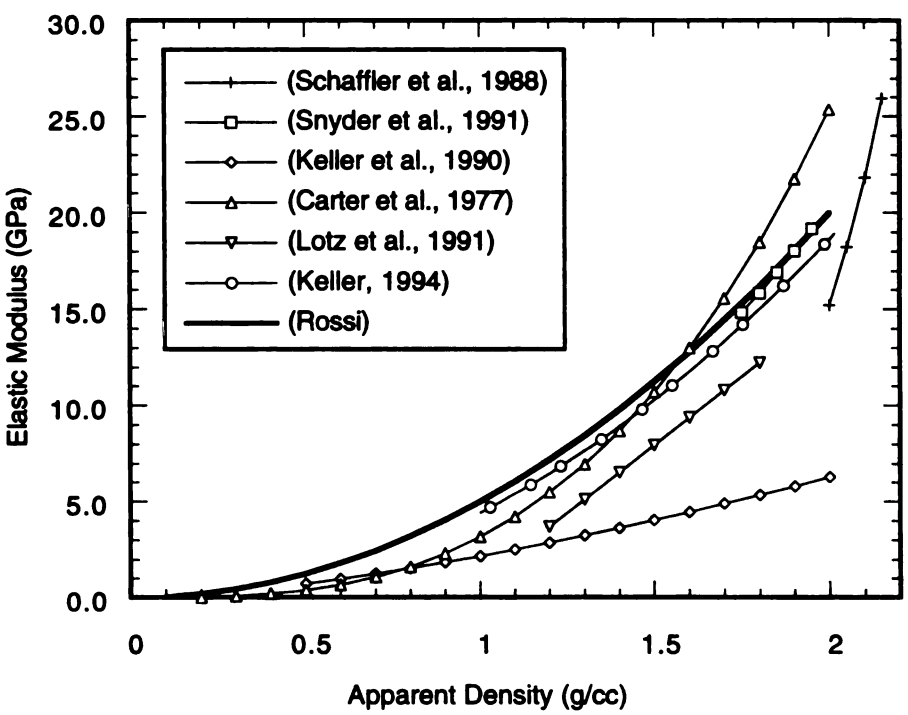


**Figure 3.1** Relationship between bone modulus and apparent density

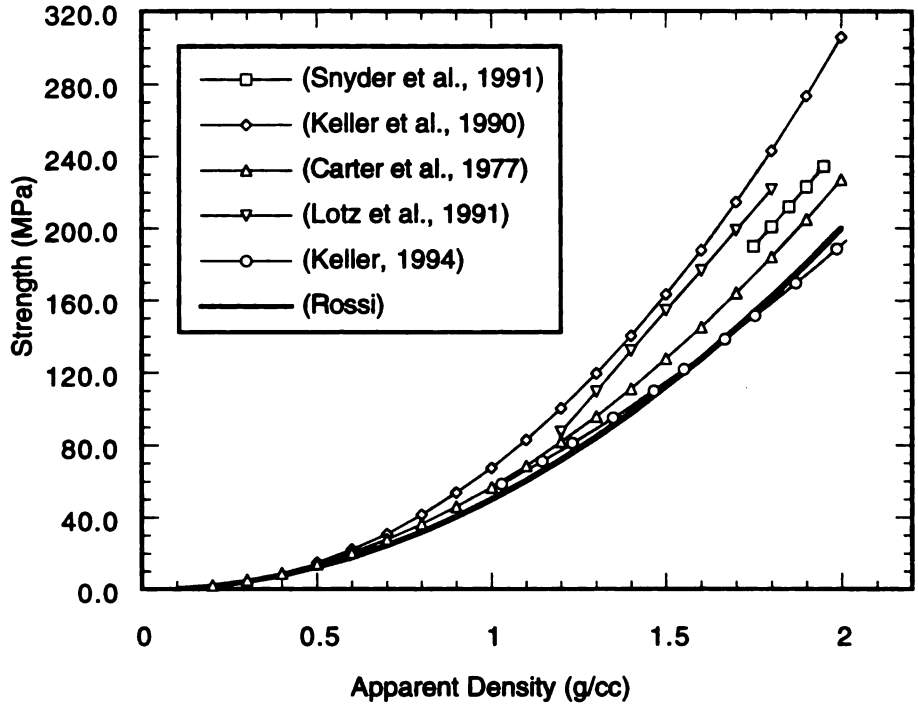


**Figure 3.2** Relationship between bone strength and apparent density

## *Computed tomography*

Quantitative Computed Tomography (QCT) is a non-invasive, three-dimensional imaging technology with densitometric capabilities. Through the rotation of x-ray sources and detectors, linear attenuation coefficients are determined at each pixel in a particular slice and are indicative of the material densities.

The use of QCT for bone densitometry has several sources of error, such as beam hardening, material inhomogeneity, and scanner drift. Beam hardening effects, which are caused by the preferential absorption of lower energy

photons, can be reduced by scanning relatively uniform cross-sections of similar material types. Material inhomogeneity effects in bone densitometry are aggravated by the presence of bone marrow fat and tend not to be significant with cortical bone. The effect of scanner drift is mitigated with the use of a calibration phantom. Provided that the proper methodologies are employed, the accuracy of densitometry for cortical bone is on the order of 2%, with reproducibility better than 1% (Cann, 1988).

To determine the utility of bone densitometry for clinical use, many studies have investigated the implications of low bone mineral density for the risk of vertebral body failure and femoral fracture. Reviews by Faulkner et al. and Hayes et al. summarized the status of the research in this area (Faulkner et al., 1991; Hayes et al., 1991). It was reported that the frequency of age-related fractures of the hip and spine increases as bone mineral density falls below certain thresholds; however, the overlap in fracturing and non-fracturing patients made many of the findings inconclusive. With both geometry and density information provided by QCT, the obvious next phase of research was to explore three-dimensional modeling of bone in order to determine strength and ultimately risk of fracture. Such models required a knowledge of geometry, material properties, and loads on the bone. QCT cross-sectional geometry was directly available, but relating bone densitometric data to mechanical properties proved more problematic. A study by Snyder and Schneider tested diaphyseal cortical bone in three-point bending, but could not find significant correlations between CT numbers and material properties due to the small range of material properties investigated (Snyder and Schneider, 1991). However, a recent study on cortical bone from the equine metacarpus found that QCT-derived $K_2HPO_4$ equivalent density proved to be an excellent estimator of dry density, elastic modulus, yield stress, and ultimate stress ($r^2$ values between 0.92 and

0.95) (Les et al., 1994). Though this study involved non-human bone, it was the first to demonstrate a significant relationship between QCT data and bone density for cortical bone. Its other findings regarding the strong dependence of material properties on bone mineral density are consistent with the findings in human studies, and the inclusion of material property variation in bone modeling techniques would seem justified.

There have been several studies of whole bone strength involving QCT. Esses et al. tested eight intact femurs in a gait loading configuration (Esses et al., 1989). They found the average CT data from the subcapital region correlated to the ultimate fracture load applied under *in vitro* conditions ($r^2$ = 0.64). A similar work by Lotz et al. found a very high positive correlation ($r^2$ = 0.93) between fracture load in a fall loading configuration and average CT values in the intertrochanteric region multiplied by cross sectional area (Lotz and Hayes, 1990). A two-part study by Lotz et al. investigated fracture prediction for the proximal femur using finite element models (Lotz et al., 1991; Lotz et al., 1991). In Part I, the researchers found excellent agreement between *in vitro* failure data and linear models of two cadaveric femora. Both the onset of structural yielding and the load at fracture were predicted for the two femora tested. In Part II, they used nonlinear material properties for both trabecular and cortical bone, and once again found excellent agreement between model predictions and *in vitro* fracture data. They concluded from these studies that while nonlinear models provided insight into events preceding fracture, linear models may be adequate for fracture prediction.

The developments described in the preceding pages outline research efforts into understanding bone as a structural material and applying that understanding to clinical issues. At the fundamental level, studies have investigated the material properties of human bone. By involving CT imaging

technology, the research advanced to the level of determining material properties *in vitro* and finally to constructing three-dimensional models. These models show promise of demonstrating whole-bone fracture strengths with the potential clinical application of predicting fracture risk. From this vantage, the current investigation sought to develop accurate models of bones containing simulated metastatic defects.

# Chapter IV

## Research methodology

A primary objective of the present study was to determine the effects of using CT scan data in the finite element (FE) modeling of human femoral shafts. By investigating both intact femoral shafts and shafts with simulated metastatic defects, the study was designed to evaluate the mechanical effects of defects and validate FE model predictions of cortical bone strength.

The experimental component of the study involved six matched pairs of femoral shafts. One shaft of each pair was left intact, while the contralateral shaft was given a hemispherical defect (6, 11, or 16 mm in diameter). Computed tomograghy (CT) scan data was collected for all shafts for use in FE modeling of bone strength. Mechanical testing of the femoral shafts in four-point bending was delayed until after all FE analyses had been performed.

The theoretical component of the study involved three types of FE models for each shaft. The first model was a homogeneous cylindrical structure with a hemispherical defect having dimensions based on shaft diameter and drill bit size. The second model used the CT scan data for truer geometrical contours, but material properties remained homogeneous. The third model used the CT scan data not only for the generation of model contours, but also for the application of heterogeneous material properties. All models were analyzed, and the results were used to predict failure loads of the experiment.

The failure loads ascertained in mechanical testing were then correlated to model predictions for each type of model. The strength of the correlations were used to test the hypothesis that increasing model sophistication (i.e. more accurate bone geometry and heterogeneous material properties) leads to more precise predictions of bone strength.

## *Specimens*

The study required 6 matched pairs of human femoral shaft at least 16 cm in length from adults over 25 years of age (**Table 4.1**). The preponderance of specimens from the male gender was an unfortunate consequence of limited bone availability.

| Specimen Pair | Patient Age | Patient Sex | Defect Size |
|---|---|---|---|
| 1 | 41 | Male | Medium |
| 2 | 44 | Male | Small |
| 3 | 53 | Male | Large |
| 4 | 43 | Female | Medium |
| 5 | 74 | Male | Small |
| 6 | 33 | Female | Large |

**Table 4.1** Specimen information for bones tested in flexion

The bones were harvested within 24 hours of death and frozen at -80 degrees Celsius; subsequent storage was at -20 degrees Celsius. Evidence has shown that freezing and thawing cortical bone does not significantly affect

its mechanical properties (Fedlin and Hirsch, 1966). The bones were inspected for evidence of previous fracture, disease, and other defects to ensure that there were minimal outside factors influencing the strength of bone. Additionally, serologies, x-ray, and cause of death were noted to ensure the safety of the investigators.

## *Specimen preparation*

To ensure that the FE models represented the precise geometry and loading conditions used experimentally, it was important that the specimens be positioned in the servo-hydraulic loading device in a known loading configuration. To this end, the femoral shafts were cut to 16 cm in length and potted in polymethylmethacrylate (PMMA) leaving 12 cm of exposed shaft. Before potting, the soft tissue and cartilage was removed from the bone shaft in order to improve the strength of the interface between bone and cement. During the potting process, the bones were kept moist to avoid the deleterious effects of dehydration. The potting fixture (**Figure 4.1**) used a solid bar connecting the two pots to maintain alignment, ensure distancing, and provide the spacing required to have the point loads on the mechanical testing device contact the bone simultaneously. The dimensions of the blocks were selected to distribute the loads over the PMMA and provide enough material to diminish stress concentration effects. Having a block of PMMA on the ends of the shaft provided a permanent coordinate system with respect to the femur for the purpose of accurate modeling and provided torsional restraint during mechanical testing.

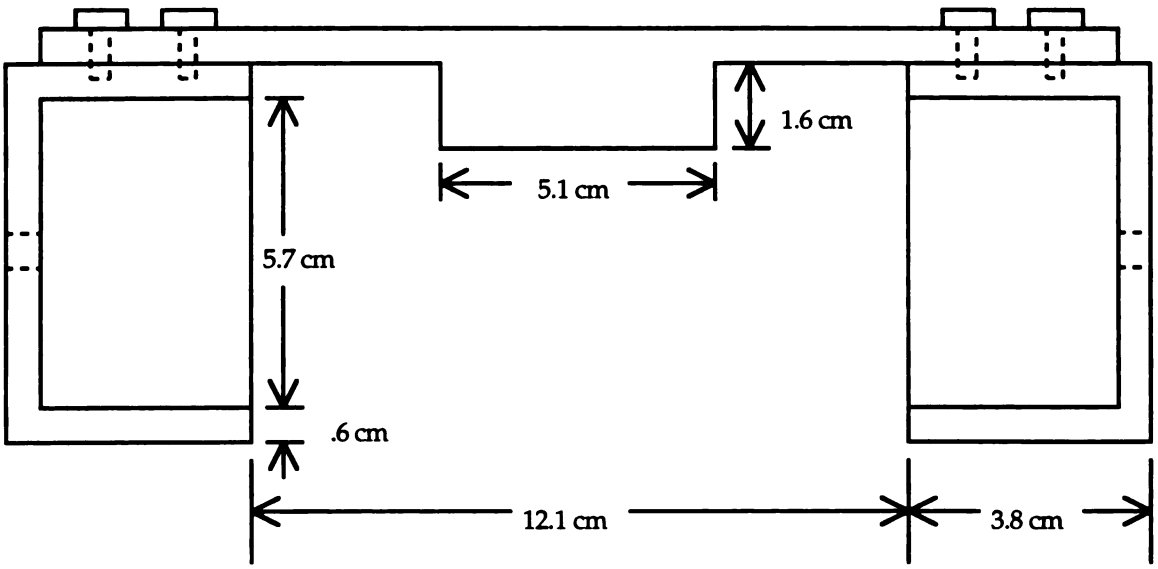


**Figure 4.1** Cross-section of fixture used to pot bone shafts

A hemispherical defect, 6, 11, or 16 mm in size, was burred into one of each pair of potted femoral shafts; these defect sizes corresponded roughly to 20%, 40%, and 60% of the bone diameter. The defects were placed on the lateral aspect of the anterior surface, which was the surface experiencing tension in the four-point bending experiment. The compressive point loads were applied to the posterior medial surface, chosen for its relatively planar contour. The fact that the bone bows in the same direction as our testing mode implies that the bone naturally experiences this loading mode *in vivo*.

## *CT imaging*

A bone and the contralateral bone containing a defect were simultaneously processed for CT scanning. Each bone was placed within a container, and the container was filled with distilled water to reduce artifacts caused by the

interface between air and bone. The potted ends were taped within the container to avoid movement of the bone during scanning. The container was then placed within another container to satisfy biosafety requirements for the transport of potentially infectious tissue.

The CT scanning was performed using the GE 9800 Quick Scanner at California Advanced Imaging, San Francisco. A Cann Genant phantom was included in each scan for calibrating each slice in terms of $K_2HPO_4$ equivalent densities and mitigating the effects of scanner drift (Cann and Genant, 1980). Scout views (AP and lateral) and a CT slice through a potted end allowed for the alignment of the shaft within the scanner, using the PMMA blocks for reference planes. Careful positioning was required because the alignment of a bone within the scanner determined the direction of loads in the finite element models. CT scan slices, 1.5 mm in thickness, were taken for the 75 mm central region of the bone, a region which included the interior two compressive load points. The scans were obtained using established parameters for bone densitometry (80 kVp, 280 mAs, 320 x 320 matrix, 1.078 mm pixel size, and 120 mm table height).

## *Formulation of FE models*

The objective of this research was to determine the utility of CT scan data in the modeling of human bone strength. To this end, three different finite element models were generated for each specimen. The first model (Model I) was based on simplified geometry with bone shafts represented as cylindrical tubes and defects as hemispherical cavities. Material properties were assumed to be linearly isotropic and homogeneous throughout the specimen in agreement

with models that have been done in previous studies (Hipp et al., 1990; Hipp et al., 1989). The second model (Model II) used CT scan data to create a model with more realistic bone geometry, once again employing linear and homogeneous material properties. The third model (Model III) not only used the CT contouring data to represent the bone geometry, but also ascribed heterogeneous material properties to elements within the model using CT numbers obtained from within the bone.

The procedure for generating a finite element model was similar for each of the three models and employed a methodology developed at our lab (Keyak et al., 1993; Keyak et al., 1990; Keyak and Skinner, 1992). The first step was to derive the endosteal and periosteal contours for each CT scan slice of a particular bone shaft, using an edge detection algorithm developed by Seitz and Ruegsegger (Seitz and Ruegsegger, 1983). Based on recommendations in the literature, the CT number threshold used to determine the presence of bone was 1600, the average between the CT numbers for water and cortical bone (Sumner et al., 1989). After establishing interior and exterior contours for all CT scan slices within a shaft, the CT numbers of the voxels within each slice were calibrated to $K_2HPO_4$ equivalent densities. The Cann Genant phantom contained regions of known $K_2HPO_4$ densities (0 to 200 mg/cc), allowing for the direct conversion of CT numbers to equivalent density. Typically, these calibration curves are not extended to the densities of cortical bone; however, recent work has shown that this extension can be done without an appreciable loss in accuracy (Les et al., 1994). Using the bone contours, calibration data, and original CT data, a finite element input file was generated which included node, element, and material definitions.

The software for generating finite element meshes used CT scan-derived bone contours to determine where to establish 1.5 mm cube elements. Surface

elements often overlapped contours and included both bone and non-bone voxels. All model types allowed for weighted averaging of material properties in elements which extended beyond the region enclosed by the contours. For the cylindrical geometry of Model I, circular contours were used whose dimensions were based on average midshaft vertical and horizontal diameters. Material properties for the two homogeneous models (I and II) were based on values reported in the literature; a Young's modulus (E) of 20 GPa and a tensile/compressive strength (S) of 200 MPa were assigned to all interior elements (Reilly and Burstein, 1975; Van Buskirk et al., 1981). Assigning heterogeneous material properties in Model III required a series of equations to convert the calibrated CT scan densities to basic material properties (**Equation 4.1**). This was achieved by converting the $K_2HPO_4$ equivalent density ($\rho_{QCT}$) of each voxel to an ash density ($\rho_{ash}$) according to a linear relationship found in the literature (Les et al., 1994). Ash densities were then converted to moduli and strengths using the simple power relationships shown in the equations. Chosen for their simplicity more than correctness, these relationships approximated the empirical relationships found in previous studies (Carter and Hayes, 1977; Keller, 1994; Keller et al., 1990; Lotz et al., 1991; Schaffler and Burr, 1988; Snyder and Schneider, 1991). Simplified relationships seemed appropriate considering the similarity in the literature data despite having variable loading configurations, bone origins, and density ranges (**Figures 3.1** and **3.2**). The material properties of the voxels within each element were finally averaged to determine the individual element material definitions.

$$\rho_{ash} = 1.22\rho_{QCT} + 0.053$$

$$E = 11\rho_{ash}^{2}$$

$$S = 110\rho_{ash}^{2}$$

| | | |
|---|---|---|
| $\rho_{QCT}$ | = | $K_2HPO_4$ equivalent density ($g/cm^3$) |
| $\rho_{ash}$ | = | Ash density ($g/cm^3$) |
| E | = | Young's modulus (GPa) |
| S | = | Ultimate strength (MPa) |

**Equation 4.1** Equations used to determine elemental material properties

Each of the three models for a given femur contained between 9000 and 15,000 linear, isoparametric, cube-shaped elements which were 1.5 mm on a side. By using the same element size and shape for all models, the effects of model geometry and homogeneity were isolated. Loads were applied to the ends of the model to simulate a 500 N load applied to each of the four points in the bending test. Because the model only included the 75 mm center section of the shaft, the four point loads were translated to shear loads and force couples applied to nodes on the model ends. The loads were added to the input file, and the model was analyzed using ABAQUS software (Hibbitt, Karlsson, & Sorensen, Inc., Pawtucket, RI).

With the completion of each FE analysis, the resultant von Mises stress distributions were examined for general characteristics. More significantly, factors-of-safety were calculated for each element within a model by dividing strength by the Von Mises stress of that element. This resulted in a distribution of factors-of-safety with the lowest factors indicating elements at high risk of

failure, whether from high stress or low strength. Failure was defined by the presence of eight "failed" interior elements in the center 37.5 mm of the model. Using too few elements for a failure criterion would tend to exaggerate model artifacts and using too many would tend to neglect stress concentration effects; "eight" was the number of elements touching a single interior node and seemed like a good compromise. A sensitivity analysis would later indicate the importance of this initial selection. The region observed for "failed" elements was the central 37.5 mm, which included most of the 51 mm between the two interior load points. This span was selected to avoid the influence of the interior load points on the failure analysis. While limiting this span would not have had any effect on failure prediction for bones with defects, it may have had some effect for whole bones.

To apply the eight-element definition of failure, the highest factor-of-safety of the eight was used as the global factor-of-safety for the model. Multiplying the global factor-of-safety by the 1000 N applied load produced a predicted failure load for the whole specimen. These failure loads were tabulated for the three models of each of the 12 bones for comparison with the mechanical testing results.

## *Mechanical testing*

After finite element analysis had been performed and failure predictions had been made, each femoral shaft was mechanically tested in four-point bending using a servo-hydraulic mechanical testing machine (Bionix 858 Test System, MTS, Eden Prarie, MN). Four-point bending was chosen as the loading modality for this study because of its relevance and simplicity. As for relevancy,

flexural studies have been performed by other researchers, providing an important basis for comparison (Hipp et al., 1989; McBroom et al., 1988). Regarding simplicity, flexural experiments are relatively easy to perform and do not require complex FE models to handle their primarily uniaxial stress state.

Throughout mechanical testing, specimens were carefully handled following extensive biosafety precautions; this included the use of lab coats, gloves, area liners, masks, plastic shields, and bleach. Specimens were allowed to thaw thoroughly prior to mechanical testing. For the test, the PMMA blocks encasing the ends of a shaft were placed on the bottom two load points (separated by 14 cm), and the actuator was positioned so that the top two load points (separated by 5.1 cm) were within a centimeter of the bone (**Figure 4.2**). The position and force transducers were zeroed, and an automated testing program was employed. The actuator was slowly ramped down to touch the bone with a force of 50 N, and a data file was opened for the collection of time, displacement, and force data. The actuator continued at a rate of 0.5 mm per second until the load dropped below 50 N, an indication of fracture. The vertical loading rate of 0.5 mm per second corresponded to an approximate average surface strain rate of 0.001 per second based on geometric calculations. A strain rate of 0.001 was chosen because of its similarity to physiological strain rates experienced during human walking.

To analyze the mechanical testing data, the load-deflection curves were reduced to measures of yield, ultimate load, maximum slope, and energy-to-failure. Yield was determined by the intersection of the load-deflection curve with a line parallel to the elastic portion of the curve and offset 0.1 mm (**Figure 5.1**). In the absence of true stress-strain data, a 0.1 mm offset seemed a reasonable method for approximating structural yield. Ultimate load was simply the highest load recorded during experimental testing. Maximum slope was

calculated by using neighboring data points to the determine slope at each possible point throughout a curve; the number of neighboring data points used in the calculation was 25% of the total number of points between test initiation and failure. Determining energy-to-failure was a calculation of the areas under the load-deflection curves, based on a piecewise approximation of the area under each data point.

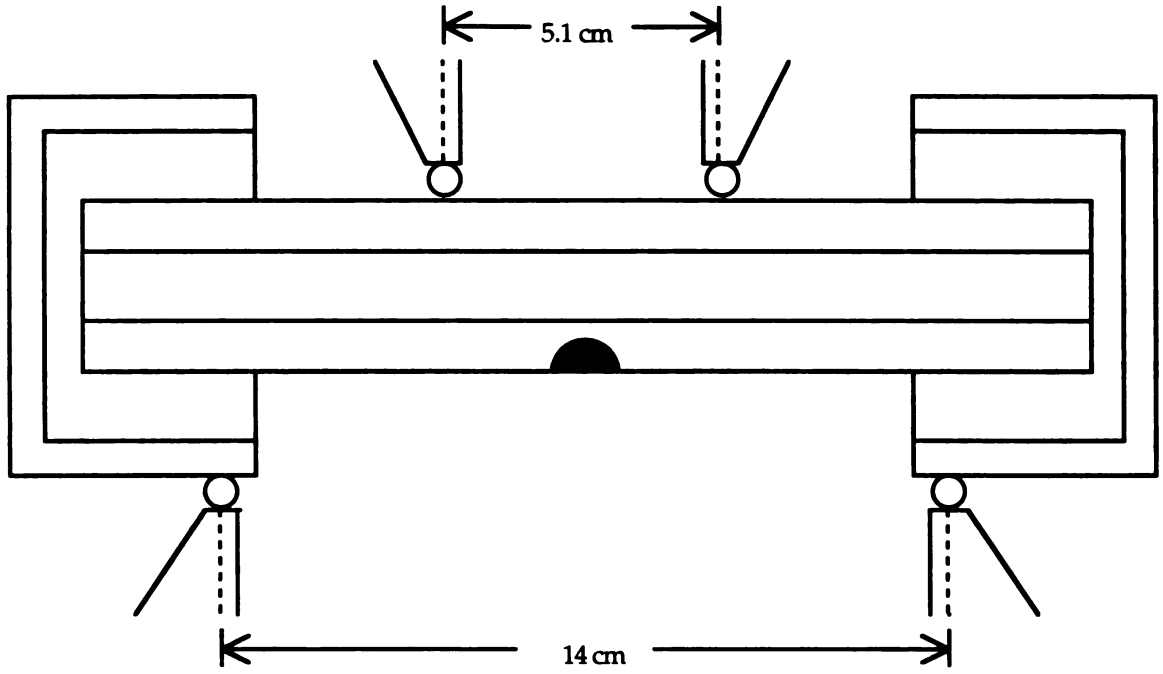


**Figure 4.2** Diagram of the four-point bending configuration

## *Analysis of results*

The procedure in this study was designed to correlate the mechanical testing data from the four-point bending of femoral shafts with theoretical failure load predictions by linear finite element models. By establishing failure criteria

for the models *a priori*, it was possible to determine the relationship between experimental and theoretical data regardless of values chosen for the specific modeling assumptions. Moreover, the use of multiple models for each bone facilitated the comparison of specific modeling assumptions without the many confounding variables typical of finite element studies (i.e. material symmetry, isotropy, plasticity, failure theory, and mesh size).

Initially, the raw testing data were analyzed for differences in mechanical behavior for whole bones and bones with defects. Paired t-tests were used to compare the maximum slopes and energy-to-failure for the two data sets. Yield and ultimate failure loads were simply tabulated for comparison with model predictions.

Correlations between the measured ultimate load and the eight-element FE model predictions were derived using a multivariate linear regression analysis for each model type. This method of analysis was chosen because this study utilized two shafts from a single donor, one with a defect and one without. The multivariate analysis accounted for the effects of specimen donor and defect presence. After the influence of defects and specimen origin were understood, the three models were compared by the strength of their correlation coefficients, a strong indication of their ability to predict fracture.

The primary focus of the bending experiment was to understand how the use of CT scan data in the FE modeling of bone shafts affected the ability of those models to determine fracture load. Because this was a first attempt to predict actual bone strength, however, additional measures were used to compare the results of this study to the work that has been performed in the past. To this end, strength reductions (defect bone strengths normalized to the contralateral intact

bone strengths) were also correlated to model predictions using linear regression analysis.

## *Reformulation of FE models and sensitivity analysis*

The finite element modeling of the flexural experiment exposed some weaknesses to certain aspects of the modeling technique. These problematic aspects included the following: (1) excessive stresses near the applied loads; and (2) errors associated with manually counting "failed" elements. Software revisions described in the following section addressed these weaknesses of the original modeling technique.

Modeling only the central region of the bone shafts necessarily complicated the loading conditions. The outer two loads of the four-point bending set-up had to be applied to the ends of the model in the form of vertical forces and transferred moments. Applying these forces to single nodes, especially the transferred moments, created stress concentrations and element distortions that caused singularity problems, possibly affecting the solution of the global model. To alleviate this concern, three planes of elements at each end were made into a stiff plate with three times the modulus and strength of ordinary cortical bone (60 GPa and 600 MPa, respectively). The loads applied to these plates were then distributed linearly over the cross-section, consistent with an idealized bending moment. The interior load points of the four-point bending models were also distributed across the top of the bone in a manner consistent with the experimental loading of the bone by a horizontal roller. These changes to the boundary conditions theoretically reduced artifacts caused by unrealistic loading conditions and restraints. A secondary benefit to distributing the loads

was that all elements within the 51 mm section between the interior loads could be considered in the failure analysis because of the absence of severe stress gradients associated with single-node loading.

The most important concern with the methodology for predicting failure was that counting "failed" elements by hand introduced error and user bias into the process. Counting was difficult due to the three-dimensional nature of the models and was further complicated by the need to exclude surface elements. Developing three-dimensional visualization software, which included the option to count clusters of elements, resolved these issues. No longer was it necessary to step through all the slices of a model and count the number of failed elements by hand; the software counted the number of contiguous elements for a given load value, automatically excluding all elements on the surface of the model.

With these modifications to the procedure, the true-geometry, heterogeneous models were reformulated and re-analyzed. The software that counted elements facilitated a sensitivity analysis on the number of elements used to determine structural failure. Correlation coefficients were derived for the different structural failure criteria in order to evaluate the robustness of the FE model predictions and to differentiate between the failure characteristics of whole bones and bones with defects.

# Chapter V

## Results

Flexural tests of six pairs of femoral shafts demonstrated differences between the load-deflection characteristics for whole bones and bones with simulated metastatic lesions. Failure load predictions by linear finite element models of these same femurs were significantly correlated with the measured ultimate loads. The precision of the predictions increased with the use of CT scan data in the FE models to assess bone geometry and heterogeneity. A parametric sensitivity analysis exposed differences in the behavior of the FE models for the two sets of bones. The specific findings are detailed below.

### *Mechanical testing*

The fracturing of cortical bone shafts was a dramatic and instantaneous phenomenon, sending bone fragments flying into the shield. The fracturing of bones with defects always occurred through the defects, resulting in transverse fracture lines with occasional butterfly fragmentation on the compressive side. The fracturing of whole bones was variable in location, but tended to be oblique in shape with occasional comminution.

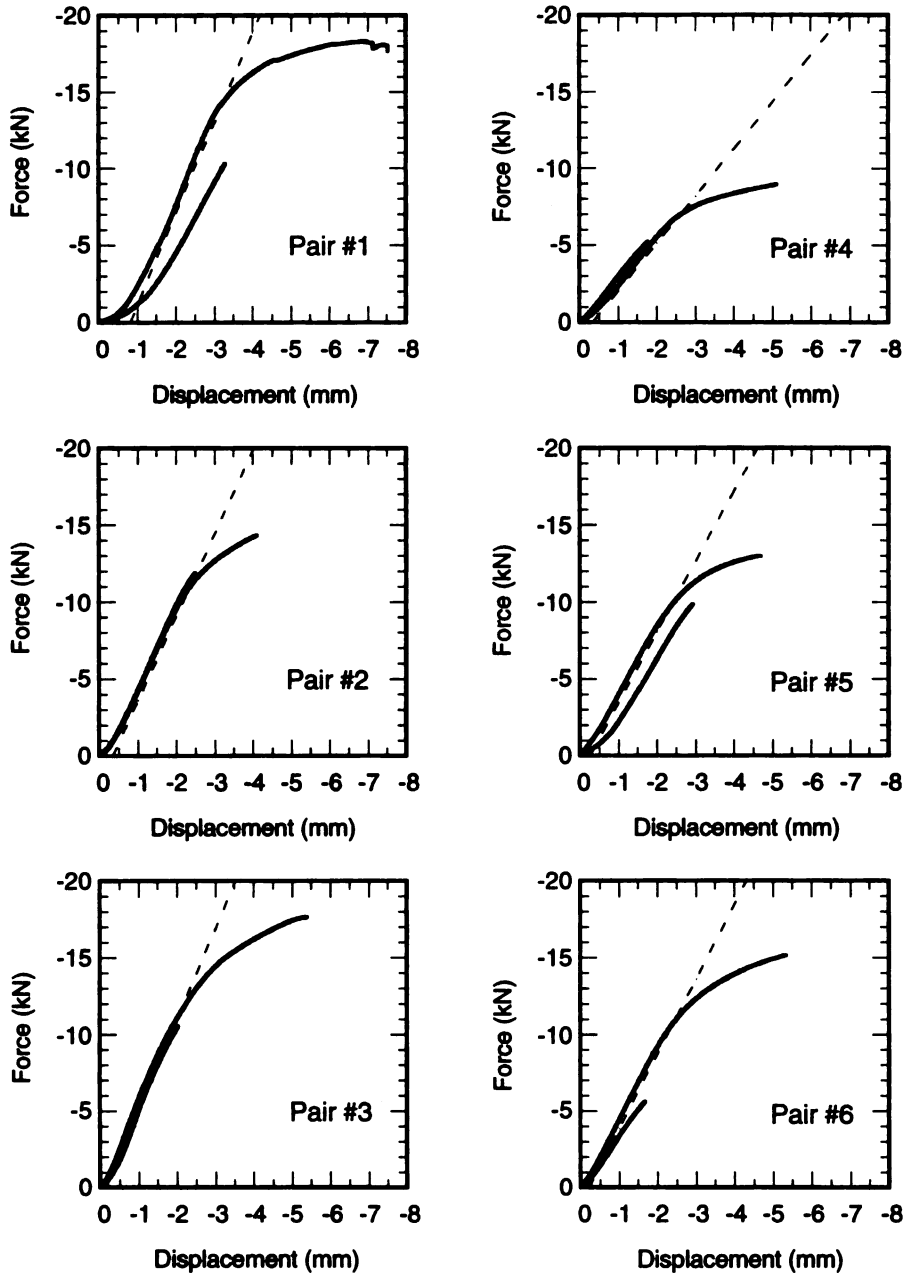


**Figure 5.1** Force-displacement curves for bones tested in bending

Scrutiny of the load-deflection curves revealed that bones containing defects underwent brittle fracture, while whole bones exhibited more ductile behavior (**Figure 5.1**). The load-deflection curves for the bones containing defects closely resembled the elastic portions of the curves for the contralateral whole bones, but fractured before any visible yielding had occurred. In fact, there was no statistically significant difference between the maximum slopes for whole bones and bones with defects ($p = 0.37$). Whole bones, on the other hand, withstood loads beyond yield and underwent extensive plastic deformation before reaching a final ultimate load. Due to this difference in toughness, the mean energy-to-failure was 50.3 N•m for whole bones and 10.0 N•m for bones with defects. The 40.3 N•m difference in energy-to-failure for the two sets of bones was statistically significant ($p < 0.01$) with a 95% confidence interval of 19.9 to 60.6. Interestingly, there was a strong relationship between yield and failure loads measured for the whole bones (**Figure 5.2**), demonstrated by the regression equation, $y = 1.35x + 0.17$ ($r = 0.96$).

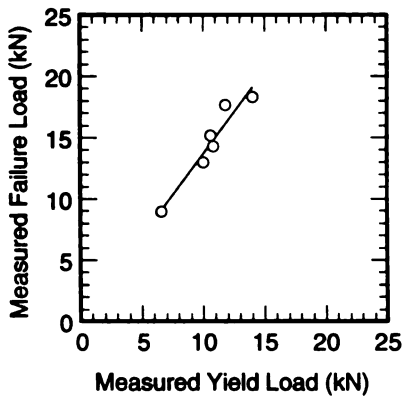


**Figure 5.2** Relationship between measured yield and ultimate load

Bones with defects failed at lower ultimate loads than the contralateral whole bones. For bones with defects, failure loads ranged from 5.2 to 11.9 with an average value of 8.9 kN. Failure loads for whole bones ranged from 9.0 to 18.3 kN with an average value of 14.6 kN. To assess bone strength as a function of defect size, the failure loads of the bones with defects were normalized to those of the contralateral whole bones, and defect diameters were normalized to the original shaft diameters. The flexural tests demonstrated a progressive reduction in strength with increasing defect size (**Figure 5.3**); a bone with a defect whose diameter was 23% of the shaft diameter retained 83% of its original strength, whereas a bone with a 67% defect retained only 37% of its original strength.

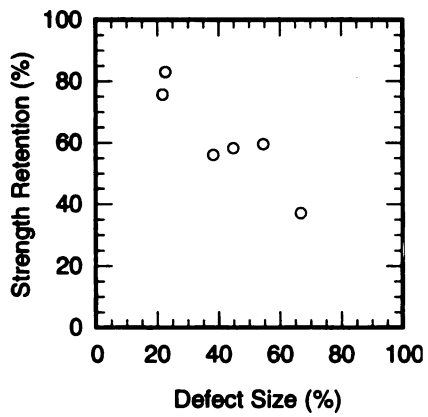


**Figure 5.3** Relationship between strength retention and defect size

## *Linear finite element analysis*

All linear FE models in this study were solved without apparent computational errors (i.e. excessive element distortions or numerical

singularities). The stress gradients for bones with small defects were more severe than those for bones with larger defects. Consequently, larger defects produced stress gradients whose effects were more distributed over entire cross-sections. Factor-of-safety distributions roughly approximated the stress profiles, with high stress regions resulting in regions of low factors-of-safety. For bones with defects, the first elements to fail were at the periphery of the defects. Whole bones initiated failure in regions of maximal tensile stress usually in areas of reduced cross-section.

| Specimen Pair (*) | | Model I Prediction (kN) | Model II Prediction (kN) | Model III Prediction (kN) | Measured Yield (kN) | Measured Ultimate (kN) |
|---|---|---|---|---|---|---|
| 1 | (W) | 22 | 21 | 18 | 14.0 | 18.3 |
| | (D) | 18 | 14 | 11 | 10.3 | 10.3 |
| 2 | (W) | 23 | 17 | 14 | 10.8 | 14.3 |
| | (D) | 15 | 18 | 14 | 11.9 | 11.9 |
| 3 | (W) | 21 | 21 | 17 | 11.8 | 17.7 |
| | (D) | 13 | 14 | 10 | 10.5 | 10.5 |
| 4 | (W) | 16 | 10 | 9 | 6.6 | 9.0 |
| | (D) | 11 | 8 | 5 | 5.2 | 5.2 |
| 5 | (W) | 21 | 17 | 14 | 10.0 | 13.0 |
| | (D) | 21 | 16 | 12 | 9.8 | 9.8 |
| 6 | (W) | 16 | 16 | 14 | 10.6 | 15.2 |
| | (D) | 9 | 9 | 7 | 5.6 | 5.6 |

* (W) whole bone, (D) bone with defect

**Table 5.1.** Failure loads found in modeling and mechanical testing

Model predictions resulting from an eight-element failure criterion and ultimate loads recorded in the experiment are presented in the table above (**Table 5.1**). Models I, II, and III predicted mean failure loads of 19.8, 17.0, and 14.3 kN for the intact bones, respectively, and 14.5, 13.2, and 9.8 kN for the bones with defects, respectively.

A multivariate linear regression analysis performed for each model type demonstrated the significance of specimen donor, defect presence, and model prediction for determining failure load. Specimen donor had no significant effect on the regression equations, and was removed from the analysis. A backward stepwise regression analysis for each model type indicated which of the remaining variables were important for predicting bone strength. For Model I, the model predictions alone had significance in the regression equation. Models II and III demonstrated a small but significant effect of the defect on the correlations, specifically on the slope of the regression equation for measured versus predicted failure load. The amount of variability explained by the inclusion of a "defect" parameter (10% for Model II, and 3% for Model III) was nominal compared to the amount explained by the model predictions. The three models types were then directly compared for their ability to predict bone strength (**Table 5.2** and **Figure 5.4**).

| Model | Equation | R Value | SEE | P Value |
|---|---|---|---|---|
| I | y = 0.69x - 0.13 | 0.76 | 2.9 | < 0.01 |
| II | y = 0.91x - 1.93 | 0.93 | 1.7 | < 0.0001 |
| III | y = 1.05x - 0.92 | 0.97 | 1.2 | < 0.0001 |

**Table 5.2.** Regression equations for failure loads

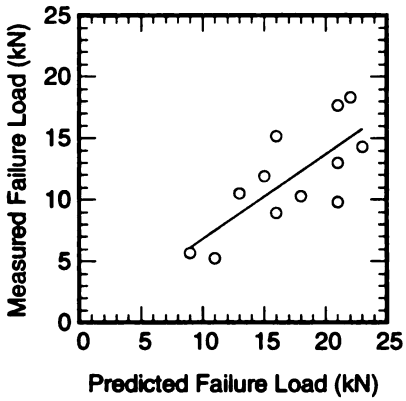


Model I. Finite element model with cylindrical geometry and homogeneous material properties.

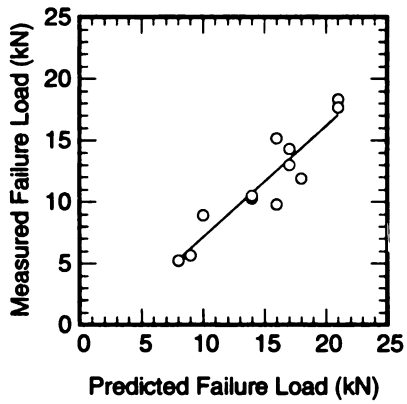


Model II. Finite element model with CT scan-derived geometry and homogeneous material properties.

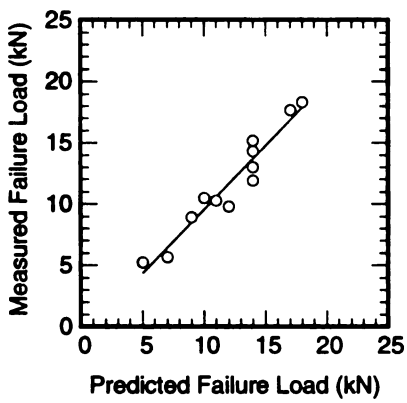


Model III. Finite element model with CT scan-derived geometry and heterogeneous material properties.

**Figure 5.4** Correlations between measured and predicted flexural loads

Strength reductions determined from the *in vitro* experiment were also correlated to predictions of strength reduction determined by the three models. Simple linear regression analysis found significant correlations for only Models II and III (**Table 5.3**).

| Model | Equation | R Value | SEE | P Value |
|---|---|---|---|---|
| I | y = 0.48x + 25 | 0.48 | 16 | = 0.34 |
| II | y = 0.81x + 21 | 0.95 | 5.9 | < 0.01 |
| III | y = 0.76x + 15 | 0.93 | 6.8 | < 0.01 |

**Table 5.3.** Regression equations for strength reductions

## *Sensitivity analysis*

The development of an automated approach to counting post-failure elements facilitated a sensitivity analysis on the number of elements used to determine failure. Linear regression analyses quantified the relationships between measured and predicted failure strengths for failure criteria ranging from 1 to 60 elements (**Table 5.4**). The correlation coefficients showed that for each group of bones (whole bones and bones with defects), the strength of the correlations were almost completely insensitive to the number of elements used. The relationship between experiment and theory, however, was unique for the two sets of bone. This was evident from the deteriorating correlation coefficients with increasing element count for the combined data sets.

| Number of | Correlation Coefficients | | |
|---|---|---|---|
| Elements | Whole Bones | Bones w/ Defects | All Bones |
| 1 | 0.99 | 0.99 | 0.98 |
| 10 | 0.98 | 0.93 | 0.95 |
| 20 | 0.97 | 0.98 | 0.94 |
| 30 | 0.95 | 0.99 | 0.91 |
| 40 | 0.96 | 0.99 | 0.89 |
| 50 | 0.95 | 0.99 | 0.86 |
| 60 | 0.96 | 0.99 | 0.84 |

**Table 5.4** Correlation coefficients for varying "failed" element criteria

Failure load was portrayed as a function of number of elements used to determine failure (**Figure 5.5**). Failure load predictions for whole bones were relatively insensitive to the number of elements used as a failure criterion due to large numbers of elements having identical factors-of-safety. Bones with defects, on the other hand, demonstrated a higher sensitivity to failure criterion. The recruitment of elements for these bones was more gradual, initiating in the region of the defect and emanating to the surrounding areas.

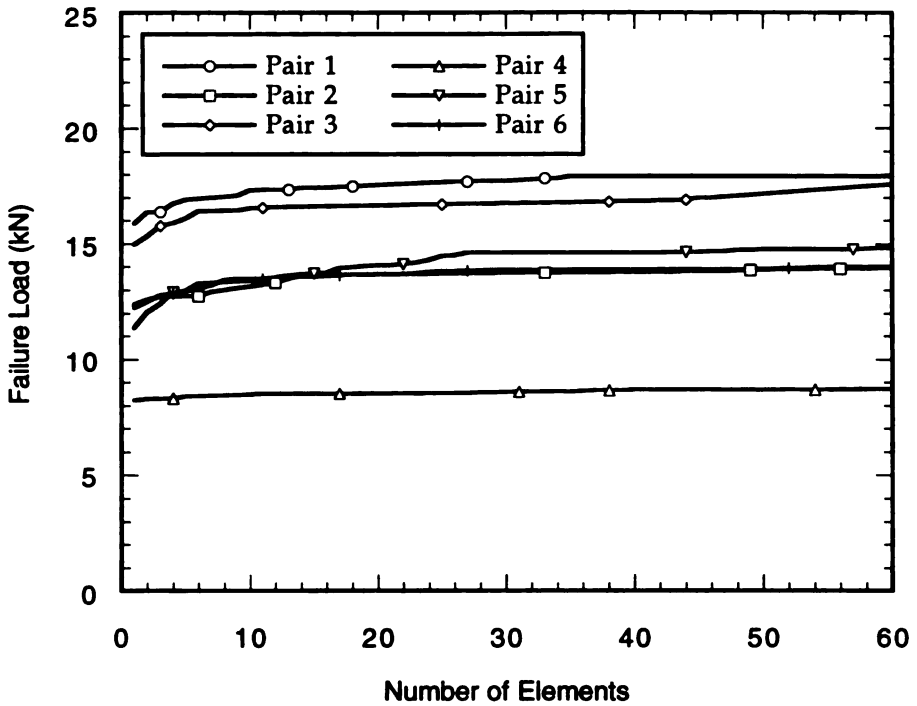


A

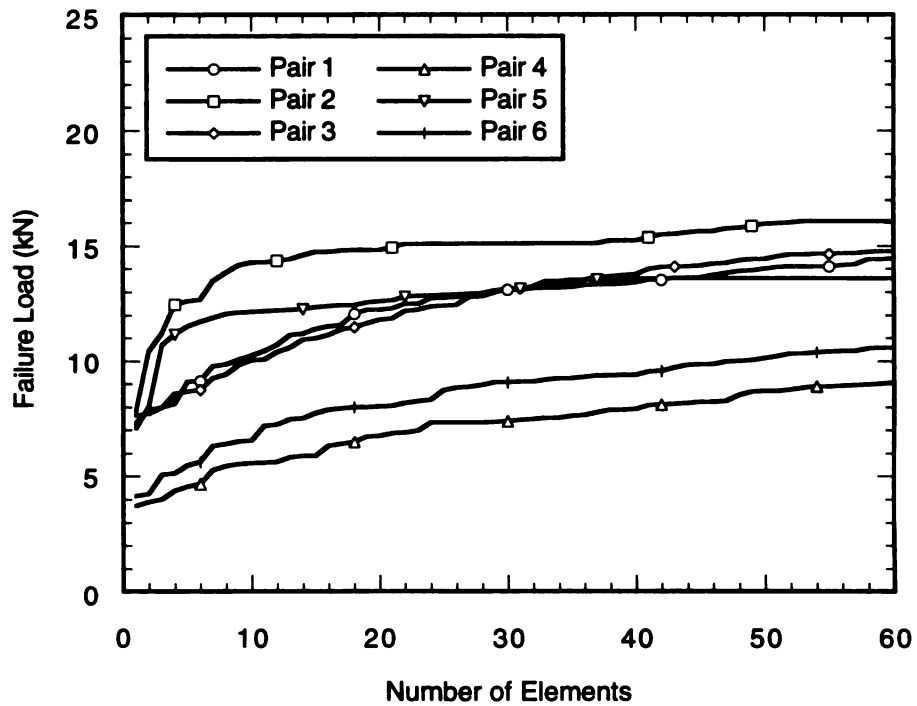


B

**Figure 5.5** Failure load versus element count for bones with defects (A - Whole bones, B - Bones with defects)

# Chapter VI

## Discussion

A major hypothesis of the present study was that using CT scan data to characterize the geometry and material properties of femoral shafts would lead to more precise prediction of strength by linear FE models. In proving this hypothesis, significant differences were found between the mechanical behavior of whole bones and bones with simulated metastatic lesions. Additionally, the precision of the resulting models provided the opportunity to explore differences in the FE modeling of these distinctly different bone geometries. The specific findings are discussed below.

### *Mechanical behavior of bones tested in flexion*

Flexural testing of bones with and without defects revealed some interesting characteristics of cortical bone failure. The shape of the breaks, for example, showed that bone preferentially yielded along transverse surfaces in tension and oblique surfaces in compression, probably because of cortical bone's relatively weak tensile and shear properties. The load-deflection curves of the tested femoral shafts demonstrated the elastic and plastic behavior of cortical bone. Interestingly, bones with defects fractured before progressing into the plastic region, while the whole bones exhibited extensive plastic deformation.

This finding suggested that a hole through the cortex introduced a stress concentration causing the region near the defect to experience post-yield stresses and initiate failure. Whole bones, on the other hand, distributed the stresses along the shaft and allowed the bone to gradually move into post-yield behavior.

The load-deflection curves for a given pair of bones were remarkable similar prior to yield but subsequently diverged in their post-yield behavior. The equivalence of the maximum slopes validated the use of contralateral bones as controls; more importantly, it suggested that the reduction of cross-sectional area was not the dominant parameter affecting structural behavior. The dramatic difference in post-yield behavior was exemplified by the 5-fold increase in energy-to-failure. Such a significant increase implied that the two most critical factors affecting structural behavior were the distribution of stresses and the post-yield behavior. Consequently, the concentration of stresses around a defect undermined the ability of the bone shaft to absorb plastic energy throughout its length.

Introducing defects into bone decreased mechanical strength. The relationship between defect size and bone strength was crudely demonstrated in the plot of strength retention as a function of defect-to-bone diameter ratio (**Figure 5.3**); McBroom et al. reported similar trends (McBroom et al., 1988). The higher magnitudes found for strength retention in the present study were probably due to the difference in defect geometry, a burred hemisphere versus their drilled hole. The fracturing of whole bones in the previous study were facilitated by a fracture initiator, which was obviated in this study by loading the bone directly and eliminating the problematic stress riser caused by potted ends. Hence, this study benefited from the direct measure of whole bone strength.

## *Predicting mechanical behavior with linear FE models*

Because of the complexity inherent to biological materials, modeling the strength of human bone requires simplifying assumptions. Previous authors assumed simplified geometry for their finite element models to reduce computational and user complexity (McBroom et al., 1988). In doing so, they were able to use one model with a specific defect-to-bone diameter ratio to represent pooled experimental data. Their linear models demonstrated significant stress concentrations around the drilled defects and severely overestimated bone strengths. It was the introduction of plasticity into their models that brought the failure predictions down to reasonable values. Unfortunately, their representative models could not be used to derive correlations between experimental and theoretical values, and their use of multiple modeling assumptions detracted from the significance of the findings. In the calculation of a ratio between the high stress around a defect and the nominal stress of an intact bone, they reported a range of values from 2.9 for the 10% defects to 6.3 for the 70% defects. This was not corroborated by either their experimental data, in which strength ratios ranged from 1.3 to 2.3 for the same defect size span, or our data, which ranged from 1.3 to 2.6 for defects spanning 38% to 66% of the bone diameter.

Another study assumed simplified geometry to correlate strength retention of femoral shafts tested in bending to the percentage of remaining cortical wall resulting from an endosteal defect ($r^2 = 0.77$) (Hipp et al., 1989). They indicated that the results of both the elastic and elastic-plastic representational models fell within the 95% confidence interval of this initial correlation. The lack of differentiation between the linear and nonlinear models resulted from the

absence of stress concentrations with endosteal defects. The minimum cortical thickness served as the only independent variable, with the model becoming a complex methodology for treating this variable. Their demonstration that the models predictions were at least as correlative as the crude geometric measurements neither validates the correctness of the model nor justifies its use as a clinical tool. Because correlations were not provided between model predictions and experimental data, it was impossible to directly compare their results with the results of this study.

In order to determine the benefit of using CT scan data in the finite element modeling of bone, Model I employed the assumptions made by previous authors by including cylindrical geometry and homogeneous material properties. Subsequent models introduced CT scan-derived geometry (Model II) and CT scan-derived material properties (Model III) to allow for direct comparison to the idealized models. The cylindrical geometry employed in this study was slightly different from that of previous studies (Hipp et al., 1989; McBroom et al., 1988) in that the contour space was subdivided into cuboidal elements, making it unreasonable to evaluate of stresses directly at the surface. This mitigated the presence of high stress gradients near defects and decreased the concomitant failure load prediction. Despite these inaccuracies, the use of cuboidal elements enabled the direct comparison of models with idealized geometry to models with CT scan-derived geometry. Moreover, the use of cuboidal elements in the CT scan-derived models allowed for high-resolution models to be achieved with minimal user involvement.

The correlations between measured failure loads and model predictions demonstrated significant relationships for all three types of models. Increases in the correlation coefficients were achieved with each increase in model sophistication. Models II and III explained 86% and 93% of the variability,

respectively, in the measured flexural strengths of all bones, a significant improvement over 57% for Model I. These improvements in precision did not include the effects of the defect parameter on the regression equations; otherwise, Models II and III could have accounted for 96% and 97% of the variability, respectively. The use of CT scan data for the determination of geometry and material properties unequivocally improved the precision of FE model strength predictions. Increasing model sophistication brought improved accuracy improved as well. Model III demonstrate remarkable accuracy with its slope of 1.05 and intercept of -0.92. This model's accuracy must be interpreted carefully, for it can only be generalized to the conditions of the experiment and the particular modeling assumptions employed; however, it is promising that accuracy improved with the more complex models.

Strength reduction caused by the introduction of defects, not actual strength, was the variable of primary interest to previous authors (Hipp et al., 1989; McBroom et al., 1988). Focusing on this variable made the accuracy of the model irrelevant because of the normalization of theoretical and experimental values. Normalization was claimed to reduce the effects of geometry, material properties, and boundary conditions on the quality of the results. These authors showed, however, only that a relatively crude geometric parameter, whether a defect-to-bone diameter ratio for a transcortical hole or a minimum cortical thickness for an endosteal coring, correlated to strength reduction. The present study derived actual correlation coefficients between measured and predicted strength reductions. The models with idealized geometry faired poorly in this study, despite being generated with specific dimensions for each bone. It became evident from actual bone cross-sections that cylinders are poor representations of bone geometry. Models II and III yielded much better correlations for strength reduction than Model I, though not quite as strong as

the correlations between actual and predicted strengths. As stated by previous authors, normalizing to whole bone strength may reduce the effects of faulty modeling assumptions and improve *accuracy*; however, calculating strength reduction actually compounds the errors associated with whole and defective bone strength predictions and diminishes *precision*. Normalizing the strength data reduces systematic error, a type of error which does not influence correlation coefficients. The compounding of error associated with the strength reduction calculation and the significant effect of non-systematic error may explain why the correlation coefficients for strength reductions were slightly reduced when compared to the correlation coefficients for actual strength.

The fact that linear FE models predicted the strength of whole bones is significant in light of recently published results (Stromsoe et al., 1995). They performed three point bending experiments on whole bone shafts and found reasonably good correlations between mechanical strength and each of the following parameters: QCT mass (density x slice area), DXA density, and DXA content (areal density x slice area). These were correlated at four geographic sites and their coefficients ranged from 0.60 to 0.79. They did not find good correlations between QCT density and mechanical parameters, most likely because of the absence of geometric information in a density measure. Their study derived over 50 correlations (a feature which necessarily weakens statistical power), all of which were significantly poorer than those found for the two CT scan-based models of this study. These results suggest the benefit of a fully automated finite element technique that uses CT scan data for geometry and density information.

Comparing the models of this study to models done by others understates the significance of the findings. Unlike the models done by previous investigators, the models of this research account for irregular and changing

cross-sectional geometry and material heterogeneity. The methodology can potentially be extended to bones whose defects manifest odd geographies, moth-eaten borders, or permeative qualities. This marks a significant step toward developing a useful clinical tool.

## *Sensitivity analysis*

The parametric variation of the number of elements used to determine failure resulted in consistently high correlation coefficients for both sets of bones (whole bones and bones with defects). Combining the data sets, however, resulted in the deterioration of the correlation coefficients with increasing number of elements. This divergence in the regression equations for the two data sets was indicative of the differences in stress distributions experienced by the two geometries. Whole bones demonstrated an instantaneous failure of large numbers of elements, consistent with the fact that a relatively uniform shaft was tested in flexion. Bones with defects had small clusters of failed elements originating near their defects, an obvious consequence of the reduced cross-sections and stress concentrations associated with defects. The excellent correlation coefficients found for the combined data sets in the previous chapter were due to the fortuitous choice of an eight-element failure criteria. This does not mitigate the significance of the previous findings, as they were meant to show differences in modeling assumptions. In fact, Model I produced poorer correlations regardless of whether the data was pooled.

The implications of the results of this sensitivity analysis went beyond suggesting the robustness of the modeling technique. They also partially explained the differences between the load-deflection curves for whole bones

and bones with defects. With their relatively uniform cross-sections, whole bones subjected to four-point bending experienced high stresses along the surface furthest from the neutral axis throughout the entire high-moment region. This implied that a large region of bone began to yield at the same time and explained the insensitivity to the selection of a failure criterion. Moreover, equilibrium and compatibility equations for the bending of a uniform shaft make it possible to extract stress-strain data from a load-deflection curve. It was therefore not surprising that the shape of the load-deflection curve for whole bones resembled the stress-strain curve found for cortical bone, with its elastic and post-yield regions. The bones with defects, on the other hand, had a geometric irregularity and the concomitant irregularity in the stress distribution. The region surrounding the defect experienced higher stresses due not only to a reduced cross-section but also to the presence of abrupt geometrical changes (i.e. stress concentration). These concentrated stresses imply that a small region of bone experience post-yield stresses and subsequent failure before the rest of the shaft even reached yield. This was demonstrated by the sensitivity of the failure load predictions to number of elements used and was corroborated by the brittle load-deflection curves of the experiment.

Understanding the differences in the prediction of failure for whole bones and bones with defects is critical to developing a technique that can be generalized to predict failure of bone in all of its many normal and pathological shapes, e.g. the proximal femur, the vertebral body, and the moth-eaten shaft. The CT scan-based finite element models of this study have shown remarkable ability to predict the flexural strength of femoral shafts both with and without defects. It has been shown that given a particular geometry, the ability of the models to predict flexural failure load is insensitive to the number of elements used as a failure criterion. More complete information is needed, however,

# Chapter VII

## Alternative material assumption: nonlinearity

In the finite element modeling of human bone, most researchers assume elastic material properties, for linear models are far less computationally intense than nonlinear ones. Linear models benefit from more expeditious processing, easier data storage, and less sophisticated modeling parameters (i.e. material definitions and failure criteria). Assuming perfect elasticity for a material that is inherently plastic, however, introduces obvious limitations on the generality of the modeling technique. It is therefore important to explore the assumption of material plasticity to understand its influence on the prediction of failure in cortical bone.

In testing the robustness of the finite element method for predicting bone failure, the previous chapter exposed some significant differences in the characteristics of the failure in whole bones and in bones with defects. Whole bones exhibited an initial rapid increase in post-yield elements along the tensile and compressive surfaces. Bones with defects, on the other hand, had a more gradual increase in post-yield elements which was focused in the region near the defect. Though this distribution of elements for the two cases is intuitive, it does not completely explain the brittle-versus-ductile structural behavior for the respective groups of bones. Further discrepancies arose from increasing the number of elements for failure determination, resulting in divergent correlations for the two experimental groups. These factors seem to imply that linear

models, while predictive of failure load, do not fully describe failure behavior. For these reasons, the assumption of material plasticity became the focus of study.

## *Revised methodology*

The investigation into the effects of elastic-plastic material properties required the reformulation and analysis of the bone FE models and the comparison of these models to mechanical testing data. In order to allow plastic behavior in the models, the methodology for generating CT scan-based FE models needed modification. The basic procedure for converting CT data into a three-dimensional model remained the same; however, the assignment of material properties to elements with that model now involved converting the moduli and strengths derived from ash densities into bi-linear material properties. This conversion to bi-linear properties was based on tensile stress and strain values found in the literature (Reilly and Burstein, 1975). Reilly and Burstein reported that human femoral bone yielded in tension at 113 MPa, and failed at an ultimate stress of 133 MPa and ultimate strain of 0.038. These data implied that bone yields at approximately 80% of its ultimate strength which it achieves at about 0.04 strain. These yield characteristics were used to apply variable stress-strain curve definitions for each element within a model in the present study. Ultimate stresses were derived from density-derived modulus and strength (**Figure 7.1**). Thus, the models were both heterogeneous and nonlinear.

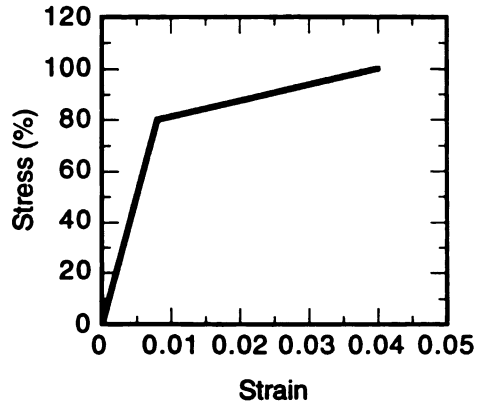


**Figure 7.1** Stress-strain relationship used in nonlinear models

The analysis of a model with a nonlinear stress-strain relationship requires an iterative process in which loads are increased incrementally and stresses are re-evaluated. For the models of the 12 bones tested in four-point bending, the loads started at zero and increased by 1 kN until a maximum load of 20 kN. The selection of a 20 kN maximum load was based on the loads seen in the actual experiment and a concern about the excessive deformations that a model could experience after yield. In its treatment of plastic material definitions, ABAQUS employed the standard Mises yield surface and associated plastic flow. This treatment assumed that the inelastic deformation rate was in the direction normal to the yield surface and that the yield surface changed uniformly in all directions with increased plastic straining (i.e. isotropic hardening).

With the element definitions and load increments redefined, the new FE models were analyzed, a process which took approximately 3 days of CPU time for each model. Each load increment for a given bone analysis resulted in stress data, producing a time course of the loads and resultant factors-of-safety.

Events in the factor-of-safety data (i.e. exceeding yield and ultimate strength criteria) were then compared to the mechanical testing data. The yield criteria used for the nonlinear models was the yielding of one, fifteen, and twenty-five elements in the region of the defect. Plastic failure was defined as the load at which the effective plastic stress within a single element exceeded 85%, 90%, or 100% of its strength. This was equivalent to allowing an element to experience 25%, 50%, or 100% of the permissible post-yield strain.

## *Results*

The correlation between the measured yield in flexural tests and first-yield predicted by nonlinear models was not as good as the previous correlations between measured ultimate load and linear model predictions (**Table 7.1**). Inspection of the data revealed that there was a definite difference in the relationship between experiment and model for whole bones and bones with defects. Increasing the number of elements used as a criterion for structural yield, however, brought the two data sets into closer agreement and improved correlation coefficients (**Figure 7.2**).

| Element Count | Equation | R Value | SEE | P Value |
|---|---|---|---|---|
| One | y = 0.68x + 3.90 | 0.83 | 1.5 | < 0.001 |
| Fifteen | y = 0.84x + 1.00 | 0.94 | 0.9 | < 0.0001 |
| Twenty-five | y = 0.94x - 0.47 | 0.97 | 0.7 | < 0.0001 |

**Table 7.1** Regression equations for yield strength

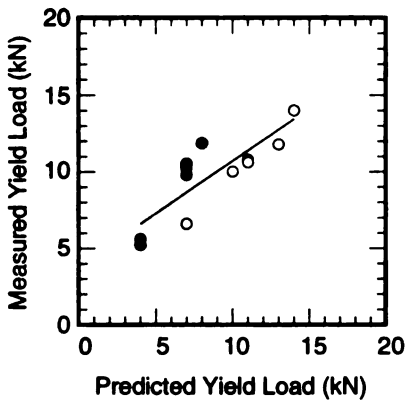


One-element yield predictions.
Whole bones (hollow circles)
Bones with defects (solid circles)

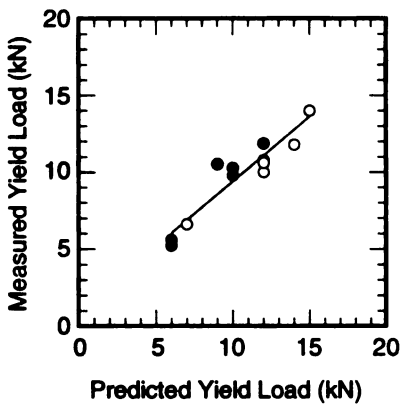


Fifteen-element yield predictions.
Whole bones (hollow circles)
Bones with defects (solid circles)

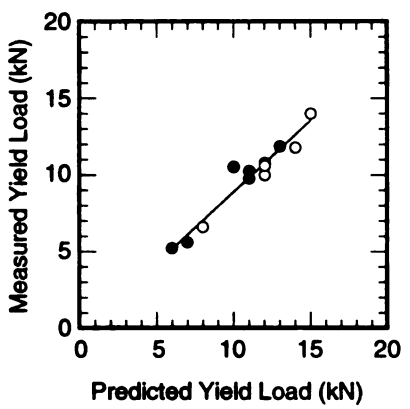


Twenty-five-element yield predictions
Whole bones (hollow circles)
Bones with defects (solid circles)

**Figure 7.2** Prediction of yield load using nonlinear models

Significant correlations were found between measured ultimate loads and the 80%, 85%, and 100% plastic failure criteria (**Table 7.2**). Two of the correlations are missing data points associated with the two strongest bones

due to an insufficient number of load increments. Even without these data points, the results were significant. The regression equations for predicting bone strength from the one-element criterion of the linear FE models and the 85% criterion of the nonlinear FE models are presented below for the purpose of comparison (**Figure 7.3**).

| Model Type | Correlation Coefficients | |
|---|---|---|
| (% strength) | Yield | Ultimate |
| Linear (100%) | 0.79 | 0.98 |
| Non-linear (80%) | 0.83 | 0.99 |
| Non-linear (85%) | — | 0.99 |
| Non-linear (90%) | — | 0.99 * |
| Non-linear (100%) | — | 0.98 * |

* missing data points

**Table 7.2** One-element failure results for linear and nonlinear models

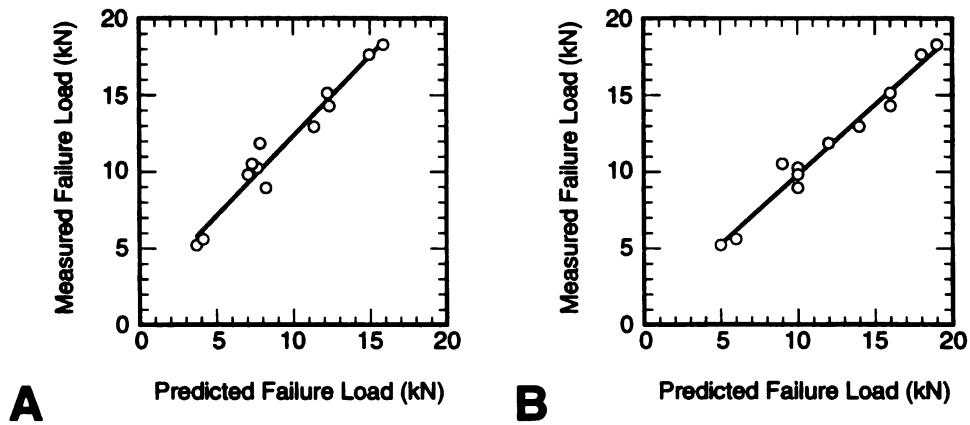


**Figure 7.3** Prediction of ultimate load by linear and nonlinear FE models

(A- Linear model, B- Nonlinear model)

## *Discussion*

The one-element yield criterion in plastic modeling was equivalent to the one-element failure criterion presented in the chapters on linear finite element models of cortical bone. Once again, the loads at which one element yielded in the models were highly correlated to the ultimate failure loads achieved by all of the bones in the four-point bending experiment ($r = 0.99$). Based on the observation that the two groups of bones – with and without defects – demonstrated different structural failure characteristics, it seemed only coincidental that the regression equations were indistinguishable for the two data sets. It seemed unlikely that linear models would consistently identify fracture load for two distinctly different geometric configurations of an elastic-plastic material.

The analysis of linear models in previous chapters employed multiple-element fracture criteria to determine failure. Though this may have demonstrated the insensitivity of the FE models to failure criteria for a given bone geometry, it had little theoretical justification within the context of linear models. In essence, counting multiple "failed" elements forced those elements which had failed at lower loads to endure stresses beyond failure. It would have been more appropriate to use only the first element exceeding the von Mises stress limit to indicate structural yield. Plastic modeling, on the other hand, does not suffer from the same limitation; after exceeding the effective yield stress, an elastic-plastic element would cease to exhibit dramatic stress increases for increasing strain. Instead, the element would strain plastically and permit the redistribution of stresses to neighboring elements. For this reason, modeling bone with elastic-plastic material properties allowed more than one yielded element to be counted.

The relationship between measured yield load and FE model predictions of one-element yield were different for whole bones and bones with defects. Differences were previously apparent from the load-deflection data for the two sets of bones; whole bones structurally yielded at approximately 70% of their ultimate load, while bones with defects failed without manifesting structural yielding. Relative to the models of whole bones, the models of the bones with defects underestimated experimental yield. This underestimation could not have been explained by the failure to use orthotropic properties and failure criteria or by a lack of smoothness in the models. All of these factors would have had the effect of reducing the concentration of stress at the defect and *increasing* model predictions. Therefore, the difference in the relationships for first yield for the two sets of bones must have been a consequence of the difference between material and structural yielding. Possibly, the appearance of structural yielding in the experiment corresponded to significantly more than one yielded element in the model.

The convergence of the two regression equations for a yield criterion of twenty-five elements provided a plausible explanation for the discrepancy between the onset of yield in whole bones and bones with defects. Possibly the "brittle" failure of bones with defects was the result of early material yielding that could not be discerned on load-deflection curves due to an insufficient volume of plastic distortion. This explanation assumes plastic material behavior for cortical bone; several important pieces of information support this assumption. First of all, the load-deflection curves for whole bones exhibited obvious post-yield behavior. By definition, the flexural test of a nearly uniform shaft resembles the underlying stress-strain relationship; thus, the changes in load-deflection slope indicated post-yield, or plastic, behavior. Material plasticity was also the most likely explanation for why bones with defects did not fail at loads

indicated by theoretical stress concentration factors. For example, the linear models in the study by McBroom et al. determined that the stress concentration factors ranged from 2.6 to 2.3 for defects ranging in size from 10% to 70% of the outer cortex diameter (McBroom et al., 1988). These theoretical calculations, however, severely overestimated the strength reductions occurring in the experiment. In fact, the magnitudes of their linear model predictions for bones with 10%, 50%, and 70% defects underestimated strengths of bones in these groups by as much 70%; this was not the case for their nonlinear models.

The assumption that cortical bone behaves plastically has direct consequences on the use of finite element modeling to interpret load-deflection data. With their nonlinear models of bone with drill holes, McBroom et al. demonstrated that yield was detected in their finite element models at only two thirds of failure load (McBroom et al., 1988). Applied to this experiment, this implies that material yielding would have begun in the linear region of the load-deflection curves, well before structural yielding of the bone. The "brittle" failure of bones with defects would, in fact, be the consequence of early but concentrated plastic yielding, imperceptible on the macroscopic load-deflection curves. Thus, the only unequivocal piece of information provided by the load-deflection data would be the structural failure load, and a phenomenologically correct FE model would require the application of a plastic failure criterion.

The failure of one element was highly correlated to the ultimate loads for the 85%, 90% and 100% failure criteria (**Table 7.2**). Demonstrating the agreement between experiment and nonlinear models was the graph of the measured ultimate loads versus the 85% plastic load predictions (**Figure 7.3**). The precision of the nonlinear models for the combined data sets further strengthened the argument for including post-yield material behavior in the FE modeling of cortical bone. Interestingly, by the time the first element had

reached 85% of its maximum effective stress, whole bones had experienced an average of 378 yielded elements, and bones with defects only 17. This difference in volume could explain the absence of structural yielding for bones with defects and the large energy-to-failure for whole bones.

The fact that nonlinear models are required to simulate mechanical behavior of cortical bone does not explain the excellent performance of one-element failure predictions from linear FE models. The strong relationship between structural yield and ultimate loads for whole bones provides only a partial explanation; at least there seems to be an empirical link between the initiation of yield, a linear phenomenon, and the occurrence of failure, a nonlinear phenomenon. The complete answer is more elusive, however. Perhaps the yielding of a single element is remarkably predictive of the subsequent failure of that element within the structure, regardless of geometry. Accordingly, whole bones and bones with defects initiated yield in flexion at about 70% of their ultimate loads, despite the fact that structural yield was only evident in the load-deflection data for whole bones.

# Chapter VIII

## Alternative loading configuration: torsion

Previous chapters have demonstrated excellent agreement between measured failure loads for femoral shafts tested in four-point bending and the predictions by both linear and nonlinear finite element models. Strong correlations were demonstrated for both whole bones and bones with simulated metastatic defects. Nevertheless, the simple bending experiment was not an adequate test of the modeling technique's generality; the flexed bones experienced high stresses mainly along the longitudinal axis, the direction of highest strength. The bones with defects did experience a slightly more complex stress distribution; however, it was impossible to separate material from geometric effects. To test the validity of the modeling technique properly, an alternative loading condition applied to the identical geometry would be required.

Modeling and testing bones in torsion provided an ideal solution, for many of the reasons described by Burstein and Frankel (Burstein and Frankel, 1971): (1) clinical relevance; (2) uniform loading along entire shaft; and (3) ease with which a constant loading rate can be applied. Most importantly for this study, the torsional testing of femoral bones with defects would apply pure shear to a geometry previously tested in bending. Now, the effects of material modeling assumptions (i.e. isotropy and linear elasticity) would manifest as changes in the relationships between model and experimental parameters.

## *Revised Methodology*

The torsional experiment involved 5 pairs of human femoral shafts (**Table 8.1**), which were harvested according to the protocol described in Chapter IV. Each shaft was potted in the fixtures used for the flexural bending experiment, with two slight modifications – the shaft was clamped at each end before potting and the length of exposed shaft was shortened by 2.5 cm. Both of these changes were made to improve the quality of the grip of the PMMA on the bone. An 11 mm diameter hemispherical defect was burred into the anterior aspect of one bone of each pair; a 16 mm defect was burred into the anterior aspect of the other.

| Bone Pair | Patient Age | Patient Sex | Femur | Defect Size | Location |
|---|---|---|---|---|---|
| 1 | 67 | Female | Right | Large | Lateral |
| | | | Left | Medium | Lateral |
| 2 | 74 | Female | Right | Medium | Medial |
| | | | Left | Large | Medial |
| 3 | 67 | Male | Right | Medium | Lateral |
| | | | Left | Large | Medial |
| 4 | 68 | Female | Right | Medium | Lateral |
| | | | Left | Large | Lateral |
| 5 | 92 | Female | Right | Medium | Medial |
| | | | Left | Large | Lateral |

**Table 8.1** Specimen information for bones tested in torsion

CT scanning procedures were identical to those followed in the bending experiment, except that an additional slice was taken through one of the potted ends of the shaft. The CT scan pixel coordinates of the potting material would later aid in the alignment of the constructed model to the actual mechanical testing configuration. As in the bending experiment, 1.5 mm CT scan slices were taken for the 75 mm central region of each bone using the following parameters: 80 kVp, 280 mAs, 320 x 320 matrix, 1.078 mm pixel size, and 120 mm table height. In addition to their important role in the FE modeling technique, the CT scans provided the information necessary to distinguish right from left shafts and determine the placement of the defect (**Table 8.1**). Distinguishing right from left was more important than knowing the exact location of the defect; shafts from contralateral limbs required testing in opposite rotational directions because of the tendency of osteons to spiral down bone shafts (Martin and Burr, 1989).

The formulation of finite element models was similar to the most sophisticated of the linear modeling techniques employed in the four-point bending study. This involved the use of CT scan data to determine the contours of a bone, generate a three-dimensional mesh with 1.5 mm cubic elements, and assign heterogeneous, linear, isotropic material properties to all elements within the model. Once again, the conversions from CT number to modulus and strength were the second-power relationships described in Chapter IV. After the generation of the FE mesh, loading conditions were applied to simulate the torsional testing configuration. This required the careful examination of the CT data to determine the center of rotation of the model relative to the testing fixture. The edges of potting material were used as reference lines. In the potting of some bones, it was noticed that the spacer used for leveling the bone within the fixture did not center the bone accurately in the direction formerly

used to apply the bending loads. Re-centering in this direction was accomplished by relocating the center of rotation in the model, thus determining the amount the actual fixture needed to be adjusted within the mechanical testing apparatus. The stiffness and strength of elements at the ends of a model were defined at three times that of cortical bone (60 GPa and 600 MPa, respectively). A torque of 10 N•m was applied to each model in the counter-clockwise direction for right shafts, clockwise direction for left shafts. These loading conditions were equivalent to an external rotation of the femur, a physiologically relevant loading configuration.

The completed models were analyzed using ABAQUS software, and factors-of-safety were calculated for each element within a model using the distortion-energy theory of failure. Global failure of a model was defined as the load at which five contiguous interior elements had factors of safety below one. Previous experiments demonstrated that the yielding of the first element was most predictive of failure; the five-element criterion was considered a compromise between using a minimal number of elements and protecting against single element artifacts. The number of elements used to determine failure was determined *a priori*; a sensitivity analysis would later determine the significance of this initial selection. The predicted failure loads were then tabulated for the 10 bones in preparation for the mechanical testing.

Mechanical testing was performed on servo-hydraulic testing machine (Bionix Model, MTS, Eden Prairie, MN) under angular displacement control. The potting fixtures were mounted to the machine platens, accounting for the lateral adjustment required to center the bone. The actuator was specified to rotate 60 degrees in femoral external rotation at a rate of 1 degree per second. Data was collected at a frequency of 200 Hz for the entire duration of the experiment, and peak torques were recorded. Simple linear regression

analysis was used to compare ultimate torques occurring in the mechanical testing to those predicted by the linear FE models.

## *Results*

Using the five-element failure criterion, the FE models demonstrated torsional failures at torques ranging from 32 to 251 N•m. Failed elements within the linear FE models clustered at the periphery of the defects. The mechanical testing of shafts in torsion resulted in spiral fracturing through their defects. The shape of the torque-angle curves exhibited brittle failure characteristics (**Figure 8.1**), with ultimate torques ranging from 19.9 to 122.7 N•m.

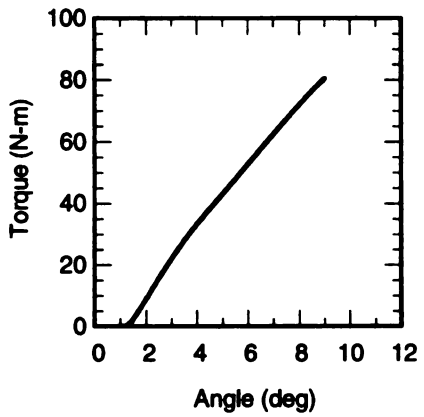


**Figure 8.1** Typical torque-angle curve for a bone tested in torsion

(Right bone specimen from pair 4)

In four of the torsional tests, the potting material cracked slightly, resulting in the appearance of artifacts in the torque-angle curves. After the appearance of an artifact, the torque-angle curve usually resumed its original course; however,

in one case, slipping caused an instantaneous high torque and premature bone failure. With the exclusion of this data point, the results of the linear model analyses and the mechanical testing were tabulated (**Table 8.2**).

| Bone Pair | Predicted Torque (N•m) | | Measured Torque (N•m) | |
|---|---|---|---|---|
| | Left | Right | Left | Right |
| 1 | 171.5 | 220.0 | 92.6 | 122.7 |
| 2 | 93.0 | 82.0 | 57.8 | 44.2 |
| 3 | 251.0 | 204.0 | 122.5 | * |
| 4 | 187.5 | 152.5 | 109.6 | 80.4 |
| 5 | 37.5 | 32.0 | 21.7 | 19.9 |

* missing data

**Table 8.2** Ultimate torques found in modeling and mechanical testing

The linear regression analysis showed a strong linear relationship between predicted and measured torque at failure (**Figure 8.2**). The predicted values for failure torque were about twice those measured in the experiment ($y = 0.51x + 5.1$, SEE = 6.2, $r = 0.99$, $p < 0.0001$). Varying the number of elements used to determine failure demonstrated the considerable insensitivity of the results to the number of elements used in the failure criterion, whether or not the data was pooled (**Table 8.3**).

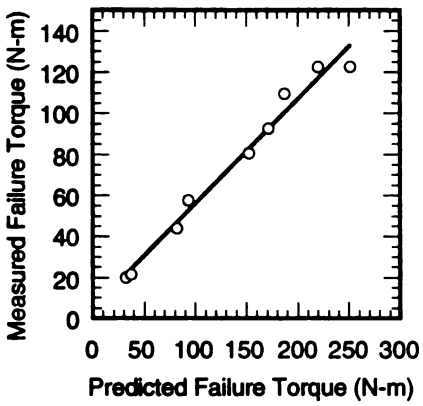


**Figure 8.2** Correlation between measured and predicted torsional load

| Number of Elements | Correlation Coefficients | | |
|---|---|---|---|
| | Small Defects | Large Defects | All Bones |
| 1 | 0.99 | 0.98 | 0.99 |
| 10 | 0.96 | 0.99 | 0.98 |
| 20 | 0.92 | 0.99 | 0.95 |
| 30 | 0.94 | 0.99 | 0.96 |
| 40 | 0.94 | 0.99 | 0.96 |

**Table 8.3** Correlation coefficients for varying "failed" element criteria

## *Discussion*

The topic of strength reduction caused by drilled defects has already been well documented in the literature (Burstein et al., 1972; Edgerton et al., 1990). The goal of the present study, however, was to use linear, isotropic,

heterogeneous FE models to predict actual torsional failure loads for femoral shafts with defects. Torsional loading produced a vastly different stress state from flexural loading and could have introduced variables that would have confounded the ability of the FE models to predict fracture. As it turns out, the models were highly predictive of ultimate torsional load with an r value of 0.99 for the five-element failure criterion. Moreover, the use of five contiguous elements was not exclusively predictive; varying the number of elements from 1 to 40 demonstrated consistently high r values.

By using simplified geometry, finite element models in the literature have obviously lacked generality; this became apparent with the inability of the FE models (Hipp et al., 1990) to explain the behavior of bones tested in torsion (Edgerton et al., 1990). The reduction of strength between a whole shaft and a shaft with a drilled defect has been the parameter typically used to compare experimental and modeling results. It is known that in both experiment and theory, the virgin bone will have 100% of its strength, with strength diminishing for increasing defect sizes; in fact, defect size alone was highly correlated (r = 0.95) with reduction in strength (Edgerton et al., 1990). The overestimation of strength reductions by linear models and underestimation by nonlinear models revealed little about what parameters are important in the modeling of femoral shafts (Hipp et al., 1990). One obvious unexplained discrepancy between experiment and model was that sheep bones demonstrated no reduction in strength with defects less than 10% of the bone diameter, while models of sheep bones demonstrated the most dramatic decrease with defects less than 10%.

Even more than in the case of flexural experiments, the stress distributions in a bone loaded in torsion is highly sensitive to local geometry. In any flexural test, the stress distributions across a cross-section are linear regardless of

shape, while torsion often creates nonlinear stress distributions. For example, maximum shear within a section is usually located on the surface closest to the center; the corners of a square cross-section sustain no shear, while dimples in a circular cross section experience high shear stresses. Moreover, holes of excessive longitudinal dimensions create an "open section" effect, severely diminishing torsional strength (Burstein and Wright, 1994). This sensitivity to geometry may explain why defects smaller than 10% did not reduce the torsional strength in sheep bones. Small defects in regions of larger cross section or along surfaces of low shear stress may not have been sufficient to decrease torsional strength. Cylindrical models would completely miss these local geometric phenomena.

The fact that the linear finite element models of this study explained nearly all of the variability in torsional strength of bones with only two defect sizes is impressive. Nevertheless, the FE modeling technique with its many simplifying assumptions may not have the accuracy required to predict failure of cortical bone regardless of geometry and loading configuration. On average, the measured torsional failure loads were half of the linear FE model predictions, which was not true for the analogous bending models. The systematic errors in the torsional models suggested the probability of faulty modeling assumptions, either in geometric or material parameters. Because of the similarity in geometry for the two experiments, inaccurate material properties or unrealistic failure criterion were the most likely reasons for differences in modeling accuracy between the two loading configurations.

One obvious reason for the discrepancy between experiment and theory was that the assumption of isotropy neglected the role of the weaker transverse properties of cortical bone. This was not an issue in bending as most of the stresses were in the longitudinal direction. However, one would expect that in

torsion, the weaker transverse properties would seriously decrease shear strength, and consequently resistance to torsional loads. The Tsai-Wu failure theory was shown to effectively handle simple cases of combined loading of bone with its orthotropic properties (Cezayirlioglu et al., 1985). According to this theory, ultimate shear stress is an independently-measured failure parameter, valued at about 50% of the tensile properties for cortical bone (Burstein and Frankel, 1971). The von Mises failure criteria employed in the linear isotropic models of the present study would predict ultimate shear stresses to be 58% of ultimate tensile stresses for the case of pure torsion. Though a likely source of error, the difference between 58% and 50% is not enough to explain the gross overestimation of torsional strengths in the experiment.

Another material assumption that may have caused additional errors in accuracy was the assumption of material elasticity. One could argue that simple elasticity was assumed for both the bending and the torsional experiments and could not have generated an additional source of error. However, cortical bone is not nearly as ductile in the transverse direction as in the longitudinal direction. The accuracy of the linear models in bending was probably dependent on the ductile behavior of cortical bone in the longitudinal direction; plastic response to stress in the region near a defect most likely resulted in higher ultimate structural loads. In the absence of shear ductility, the bones tested in torsion failed at first yield; accurate torsional models would have needed substantially lower strength values to predict the brittle structural failure of the experiment.

Though not achieving the desired accuracy, the linear models of bones tested in torsion performed extremely well. It becomes apparent from the lack of accuracy that the FE modeling technique requires further modification before it can achieve complete generality. The data suggests that applying material

plasticity and employing orthotropic failure criteria are the two most likely methods for improving the modeling technique, and ultimately increasing its accuracy.

# Chapter IX

## Building a general model

Developing a useful clinical tool was the major impetus for the research detailed in the previous chapters. Such a tool would improve the treatment protocol for patients suffering from metastatic lesions in long bones. A good understanding of the strength of femoral bones with such defects would help surgeons make prophylactic decisions aimed at averting pathological fracture. Toward this end, this research employed finite element models that used CT scan data for information on geometry and material property variation. In reliably predicting the failure loads and torques achieved by femoral shafts in mechanical testing, these models marked a significant step in research efforts to predict the strength of human femurs *in vivo*. Furthermore, the process of developing these models for fracture prediction revealed characteristics of cortical bone failure with far reaching implications for bone modeling, regardless of application. These failure characteristics can be classified as either the effects of geometry or the effects of material properties on the behavior of bone structures in both theory and experiment.

### *Geometric issues: stress concentrations*

For femoral shafts tested in either bending or torsion, the introduction of a defect into the periosteal surface caused significant reductions of strength.

Previous studies characterized these reductions in strength for both experiment and theory by comparing the strength of a shaft with a drilled hole to the strength of the intact contralateral femur (Hipp et al., 1990; McBroom et al., 1988). Their findings for three different defect sizes have been tabulated for ease of comparison (**Table 9.1**).

| Method for Determining Failure | Percentage of Intact Bone Strength | | |
|---|---|---|---|
| | 10% Defect | 30% Defect | 50% Defect |
| Flexural Experiment * | 76% | 59% | 50% |
| Linear Flexural Model * | 34% | 29% | 23% |
| Torsional Experiment ** | 100% | 55% | 37% |
| Linear Torsional Model *** | 61% | 46% | 33% |
| Non-linear Torsional Model *** | 90% | 77% | 54% |

* (McBroom et al., 1988)

** (Edgerton et al., 1990)

*** (Hipp et al., 1990)

**Table 9.1** Experimental and theoretical strength retention in femoral shafts

Assuming that cortical bone behaved as a perfectly elastic material, the reductions of strength caused by a defects in cylindrical shaft would be similar to those determined by theoretical stress concentration factors reported in engineering literature. For example, a 10% defect would have stress concentrations of 2.3 in bending and 1.7 in torsion, and a 30% defect would have stress concentrations of 1.9 in bending and 1.4 in torsion (Peterson, 1953). By adjusting these factors to account for original cross-section, they can be converted to strength retentions for comparison to those measured and

calculated in the experiments. The flexural factors-of-safety for 10% and 30% defects translate to strength retentions of 37% and 26%, respectively; the torsional factors of safety for 10% and 30% defects translate to strength retentions of 56% and 53%, respectively. Not surprisingly, these values correspond to the predictions by the linear models reported in the above table (**Table 9.1**); they are not exactly equivalent because of the difference between double and single cortex holes, and because of the difference between maximum and effective stress analyses.

The importance of describing the theoretical context for stress analysis in shafts with holes is that the behavior of bones with defects *did not* behave according to predictions based on linear failure theory or stress concentration factors. While faulty material property assumptions are the most likely cause of this incongruency, flaws in the geometric representation of bone shafts must have also played a role. For example, models of sheep bones tested in torsion could not explain the non-existent decline in strength with defects less than 10% of the shaft diameter (Edgerton et al., 1990; Hipp et al., 1990). While it was hypothesized that natural defects in the bone caused this phenomenon, it is equally likely that cylindrical models underplayed the importance of local geometry in determining the effects of small holes on bone strength. More importantly, the CT scan-based finite element modeling of the present study concretely determined that more accurate geometric representation led to greatly improved model precision. With its lack of precision for failure determination, the cylindrical model, regardless of material assumptions, could not have been expected to accurately describe the response of a bone to the presence of defect. This was especially true for torsion, a mode of loading whose stress distribution is highly dependent on cross-sectional geometry.

## *Material issues: heterogeneity, plasticity, and anisotropy*

While the effects of geometry are important in discerning differences in strength between whole bones and bones with defects, the effects of material property assumptions are more likely to explain gross inaccuracies in the modeling of bone strength, independent of the presence of a defect or the method of loading employed. In looking at the flexural and torsional strengths of femoral shafts, the present study elucidated some probable consequences of different material modeling assumptions (i.e. heterogeneity, plasticity, and anisotropy). A better understanding of the effects of different modeling assumptions would hopefully lead to the development of more general bone models that can be confidently extended to conditions *in vivo*.

The heterogeneous nature of cortical bone is easily proved. At a purely microscopic level, the microstructure of cortical bone, with its uneven distributions of pores and cement lines, would seem to cause material heterogeneity. However, this alone does not demonstrate material heterogeneity, for if the spatial frequency of these variations is high and uniform enough to be invisible to the stress distribution, the material could be considered homogeneous. For the case of cortical bone, it is macroscopic evidence that attests to its heterogeneity. The fact that appreciable density variation can be measured in cortical bone and that this density variation correlates to material behavior confirms that cortical bone is heterogeneous. Supporting these facts are the changing porosity and bone distribution with age and the hypertrophic response of bone to the presence of a metastatic lesion. Despite the ease of proving bone heterogeneity, quantifying this variability poses a challenging problem for researchers. In the present study, a second-

power relationship between CT scan-derived density and the material properties of modulus and strength was used to explain some of this variability. The extremely high correlation coefficients achieved by the heterogeneous models gave merit to the assumed heterogeneity. More importantly, it can be conjectured that its role in accurate strength predictions will only increase for cases where the heterogeneity is more pronounced. Even if cortical bone does not demonstrate significant intra-specimen heterogeneity, the application of some relationship between density and material properties could quantify differences in material properties between specimens.

The evidence for material plasticity in cortical bone is compelling. The literature discusses how bone may be considered a bi-phasic material in which the more flexible collagen combines with the stronger ground substance to provide more composite strength than either material alone would predict (Fung, 1993; Nordin and Frankel, 1989). In fact, one study postulated that only in the presence of the purely elastic behavior of collagen is the mineral substance elastic-perfectly plastic, together giving cortical bone its characteristic bi-linear stress-strain curve (Burstein et al., 1975). The importance of assuming plastic behavior in cortical bone becomes evident in the structural behavior of whole bone subjected to four-point bending; the extensive deformation occurring after yield can only be explained by plastic material behavior. Despite the obvious plasticity of cortical bone, many argue that elastic modeling is equally predictive of failure and much less computationally intensive. Because of the strong relationship between yield and ultimate strength for the mechanical testing of a uniform section, linear models are often just as predictive of strength as nonlinear models. However, these relationships between yield and ultimate failure load can only hold for a given geometry, thus limiting the generality of the modeling technique to the exact cases which have

been tested empirically. The presence of a defect, for example, causes the relatively brittle failure of shafts tested in torsion or bending. For both of these cases, the literature reported extremely poor modeling accuracy and an inability to explain the less than drastic reductions in strength caused by defects (Hipp et al., 1990; McBroom et al., 1988). The results of the present study show that a high degree of precision can be achieved in the linear modeling of flexed bones with and without defects and torqued bones with defects, provided the geometric representation is reasonably accurate. Nevertheless, the extremely different mechanical behavior for whole bones and bones with defects made the assumption of material elasticity suspect. By analyzing nonlinear models for the flexural experiment, it was postulated that assuming material plasticity showed potential for not only increasing the accuracy of the models in predicting failure, but also increasing the generality of the model to multifarious loading conditions and explaining actual mechanical behavior (e.g. structural brittleness versus ductility).

With its inherent secondary osteonal organization, cortical bone demonstrates directionality to its material behavior, discrediting the assumption of isotropy. Though the orthotropic properties of cortical bone are well documented (Reilly and Burstein, 1975; Van Buskirk et al., 1981), it remains unclear exactly how to implement this knowledge in the FE modeling of cortical bone structures. For example, one study demonstrated that model solutions were dependent not only on the inclusion of orthotropic behavior but also whether the orthotropy was aligned with the changing principal axes of the osteons along a curved bone (Ricos et al., 1996). Even if the moduli were accurately assigned to a bone model, the question remains how to apply a failure criterion that would also account for strength anisotropy. It is obvious that a multiaxial criterion is necessary. Many have noted that bone fractures on

surfaces of maximum shear for compressive loading and on surfaces of maximum tensile stresses for pure tensile or shear loading, indicating a hierarchy of failure modes which depends on directional weaknesses (Burstein and Wright, 1994; Hipp et al., 1992). One study has successfully applied a Tsai-Wu failure criterion to cortical bone specimens under combined axial-shear loading, further strengthening the argument for the assumption of anisotropic material properties and the use of a multiaxial failure theory in the modeling of cortical bone. Complications still arise with the fact that multiaxial failure theories usually define yield surfaces, which could be confounded by the additional directionality associated with post-yield behavior (Keaveny and Hayes, 1993). Having precisely modeled the strength of bones in torsion, the present study offers more evidence to justify the need for orthotropy in the modeling of cortical bone structures. The severe underestimation of the torsional strength of bone with defects, despite accurate predictions for flexural strength, can only be attributed to the anisotropy manifested by the transverse loading configuration of torsion. No doubt, the fully general FE model of cortical bone would accommodate orthotropic material properties in addition to material heterogeneity and plasticity.

# Chapter X

## Conclusion

Investigating the use of CT scan data to build models of femoral bone shafts produced many significant findings. Though the previous chapters have served to quantify these findings and extrapolate their physical significance, it is important to qualify them, placing them solidly within the context of the scientific and clinical knowledge. Understanding both the implications and limitations of the findings is essential for moving medical research toward the ultimate goal of improved patient care.

### *Research findings*

A principal goal of this research was to determine if CT scan data offered some benefit in the FE modeling of femoral shafts. To give this research additional clinical significance, shafts with simulated metastatic defects were also included in the investigation. While the effects of drilled holes in long bones had already been studied, no study had ever performed both finite element modeling and experimental testing of human bones with defects. Moreover, previous FE models of animal bones with defects all assumed a simple cylindrical geometry. In performing multivariate linear regression analysis on the ability of three model types to predict strength, the present study determined that using CT scan data to describe bone geometry resulted in marked increases in model precision, and that using it to describe geometry

and material heterogeneity brought both precision and accuracy. The correlation coefficients for predicting the flexural strength of bones with and without defects were the highest ever reported in the literature.

Within the maelstrom of data on the strength characteristics of human bone, the material property assumptions were carefully justified for the performance of the early linear models of the four-bending tests; the idea was only to compare geometry and heterogeneous modeling assumptions. These models included assumptions of linear elasticity, isotropy, and density-based heterogeneity. With the success of these models in predicting bone strength, other modeling assumptions were open to exploration. It was through the variation of number of elements used to determine bone failure and a closer inspection of the load-deflection curves that it was determined that bones with defects were distinctly different in their failure characteristics than bones without defects. Despite showing considerable robustness of the modeling technique, varying the number of elements to failure suggested that linear modeling probably could not explain the subtleties of the different failure mechanisms in whole bones and bones with defects.

The next modeling assumption to be explored was that of nonlinear material properties. By allowing plastic deformation in the region of a defect, a bi-linear stress-strain relationship would potentially explain the differences in the characteristic load-deflection curves for the two sets of bones tested in bending. It was found that nonlinear models performed quite well and provided a probable explanation for why local yielding near a defect did not translate to structural yielding on a load-deflection curve. The nonlinear models also suggested the mechanism by which bones retained a much larger portion of their original strength than predicted by presence of stress concentrations. It seems likely that including plasticity in models will play an increasingly

important role as geometries become more complex and loading conditions more varied.

Because flexural tests provide limited data on the multiaxial failure characteristics of bone, torsional experiments of bones with defects were performed. Torsional models proved to be even more precise than the original bending models; however, they did not achieve equivalent accuracy. As models were predicting strengths to be twice their empirical values, isotropy and the associated uniaxial failure theory were the most likely sources of systematic error. Based on reduced strengths in the transverse directions and an incongruency between longitudinal ductility and transverse brittleness, both orthotropic material properties and a multiaxial failure criterion may be required to characterize bone strength more accurately in such complex loading configurations. Even with its limitations, linear modeling proved to be a reliable predictor of bone strength in both bending and torsion, marking a significant step in the modeling of cortical bone as a structural material.

## *Sources of Error*

Even with the high degree of precision achieved by each of the experiments in this study, it is important to understand the limitations of the general FE modeling technique for predicting bone strength. The errors associated with faulty material property assumptions have already been described in detail. Absent a fully heterogeneous, elastic-plastic, orthotropic modeling technique, one can expect errors to always be present. Two material assumptions which were not mentioned were strain rate dependence and asymmetry, also potential sources of error. Beyond using faulty material assumptions, there are errors inherent to the biology of bone. For example, bone may manifest effects of

osteoporosis or tumor metastasis completely independent of bone density, the only parameter measured by a CT scan. Until osteoporotic or lytic bone can be more fully characterized, it will remain a mystery what variability these factors would introduce to the strength modeling process. Additionally, any *in vitro* experiment lacks the reality of a bone's interaction with its environs, including the effects of temperature, pressure, biochemical interactions, and real time bone adaptation.

Regarding the experiment itself, errors originated from each step in the process. Preparing the specimens exposed the bones to cold temperatures of the freezer and hot temperatures of the potting process, desiccating environments of the freezer and rehydrating environments of the water bath. Using CT scan data to determine bone geometry and density had a host of potential confounding variables: scanner drift, threshold selection, scanner resolution, and beam hardening artifacts. Additionally, ensuring that the bone within a scan precisely corresponded in alignment to the bone within the mechanical testing machine gave the researcher many places to err, such as within the scanner, the mechanical fixture, and the model. The formulation of the models from CT scan data created a rough-surfaced model with its cuboidal elements, necessarily eliminating surface elements from consideration in stress analysis. Because of this roughness, the accuracy of the stress distributions was completely dependent on the resolution of the model, perhaps causing errors in regions with drastic stress gradients. The physical breaking of the bone may have introduced even more errors associated with stress concentrations at load points and interface problems near the potting material (e.g. premature cracking).

Possible sources of error for the present study have been only cursorily described, because with only 4% of the variability in the experiments left

unexplained, it would be futile to quantify the myriad sources of error in search of a direction for improvement. However, many of these possible sources of error can be addressed by thoughtful modifications to the modeling technique in future experiments.

## *Future directions*

The results of the present study hold promise for the development of fracture risk criteria for patients suffering from metastatic lesions in the femur. Absent new techniques for risk determination, many patients will be either subjected to unnecessary fixation procedures or suffer preventable painful fractures. In this investigation of flexural and torsional strength, the strengths of human bones with hemispherical defects were determined theoretically with great precision. The sophistication of the modeling technique coupled with its facility allows it potentially to be extended to bone configurations of greater complexity. Before accurate models are ultimately achieved, however, there are many smaller research steps that must be taken.

Throughout the entire discussion of bone strength, many simplifying geometric and material property assumptions have been suspected of detracting from the quality of the modeling technique. Regarding geometry, increasing mesh refinement would be the obvious direction for improving model precision; with the constant advancements in computer technology, this improvement should come inexpensively. Material property assumptions will always be a source of error in modeling bone, a material with complex biological behavior. Nevertheless, discussion in the preceding chapters suggests that a fully general and accurate model would require closer approximations of the inherent properties of cortical bone, such as

heterogeneity, plasticity, anisotropy, and asymmetry. Future studies could investigate how the inclusion of closer approximations of material behavior would affect model predictions of structural behavior. In addition looking at ultimate failures, these studies of material behavior could characterize the structural stiffness and local strains of the loaded bones. Other important areas for investigation including alternate bone geometries and loading configurations.

Thus far, the focus has been on improving *in vitro* fracture prediction. Other areas for investigation become important if the FE modeling technique is to be of clinical significance. For the purpose of scientific exploration, it has been assumed throughout this research that developing a fully general model was the ultimate goal. Perhaps, clinical practice could benefit from research with less ambitious expectations. For example, results from the present study could possibly be developed into criteria for deciding on the need for prophylactic fixation. Applying engineering beam theory to the cross-section of a bone with a metastatic lesion may allow surgeons to realize the benefits of this research without the cost of expensive technologies. The poor performance of current clinical criteria warrants this search for better rules of thumb.

The value of achieving the most general model for bone strength depends on results of future clinical studies. For example, the region neighboring a metastatic lesion can be osteolytic or reactive, depending on the span of time over which the tumor has developed. Characterizing the strength of this neighboring bone becomes a confounding issue, because it is possible that density measures do not fully incorporate the demineralization associated with lytic bone or disorganization associated with reactive bone. One study applied acid to bone to approximate the structural effects of a lytic lesion with little success (Hipp et al., 1991), most likely because acid did not produce a region of

graded demineralization. The CT scan-based technique offers the capability to model bone with actual tumors, eliminating the need for a flawed simulation. Another important issue regarding the development of a clinical tool for fracture prediction involves the loading a femoral bone can expect to experience *in vivo*. Fracture prediction based on simple *in vitro* loading configurations may not satisfactorily represent the complex loading configurations of normal human activity; future research should address this issue. A final extension of this research would be the application of the FE method to other regions of bone, such as the proximal femur or the vertebral body. One study reported a 30.6% incidence of spinal metastases in patients dying from malignant neoplasms (Ortiz Gómez, 1995), a testimony to the need for other bone studies. Only one parametric FE study on spinal metastases has been done to date (Mizrahi et al., 1992).

Only after the appropriate amount of background research has been performed can a FE-based fracture criterion be introduced into the clinic. Clinical trials would be required to prove the method efficacious and justify its use. With the current fracture risk criteria so unreliable, it seems likely that the precision of the FE models using CT scan data would afford great benefits, especially with its ability to uniquely characterize bone geometry and heterogeneity. This is obviously a very exciting field in which to be doing research!

# References


1. Beals RK, Lawton GD, Snell WE: Prophylactic internal fixation of the femur in metastatic breast cancer. *Cancer*, 28(5):1350-4, 1971.

2. Bonarigo J, Rubin P: Non-union of pathologic fracture after radiation therapy. *Radiology*, 88:889, 1967.

3. Brooks DB, Burstein AH, Frankel VH: The biomechanics of torsional fractures. The stress concentration effect of a drill hole. *J Bone Joint Surg [Am]*, 52(3):507-14, 1970.

4. Burstein A, Wright T: *Fundamentals of orthopaedic biomechanics.* Williams and Wilkins: Baltimore, MD, p. 132-87, 1994.

5. Burstein AH, Frankel VH: A standard test for laboratory animal bone. *J Biomech*, 4(2):155-8, 1971.

6. Burstein AH, Zika JM, Heiple KG, Klein L: Contribution of collagen and mineral to the elastic-plastic properties of bone. *J Bone Joint Surg [Am]*, 57(7):956-61, 1975.

7. Cann CE: Quantitative CT for determination of bone mineral density: a review. *Radiology*, 166(2):509-22, 1988.

8. Cann CE, Genant HK: Precise measurement of vertebral mineral content using computed tomography. *J Comput Assist Tomogr*, 4(4):493-500, 1980.

9. Carter DR, Hayes WC: The compressive behavior of bone as a two-phase porous structure. *J Bone Joint Surg [Am]*, 59(7):954-62, 1977.

10. Carter DR, Spengler DM: Mechanical properties and composition of cortical bone. *Clin Orthop*, 135:192-217, 1978.

11. Cezayirlioglu H, Bahniuk E, Davy DT, Heiple KG: Anisotropic yield behavior of bone under combined axial force and torque. *J Biomech*, 18(61-9), 1985.

12. Cheal EJ, Hipp JA, Hayes WC: Evaluation of finite element analysis for prediction of the strength reduction due to metastatic lesions in the femoral neck. *J Biomech*, 26(3):251-64, 1993.

13. Clark CR, Morgan C, Sonstegard DA, Matthews LS: The effect of biopsy-hole shape and size on bone strength. *J Bone Joint Surg [Am]*, 59(2):213-7, 1977.

14. Cowin SC: Mechanics of materials, in *Bone biomechanics*, CRC Press: Boca Raton, FL, p. 15-42, 1989.

15. Edgerton BC, An KN, Morrey BF: Torsional strength reduction due to cortical defects in bone. *J Orthop Res*, 8(6):851-5, 1990.

16. Esses SI, Lotz JC, Hayes WC: Biomechanical properties of the proximal femur determined in vitro by single-energy quantitative computed tomography. *J Bone Miner Res*, 4(5):715-22, 1989.

17. Faulkner KG, Gluer CC, Majumdar S, Lang P, Engelke K, Genant HK: Noninvasive measurements of bone mass, structure, and strength: current methods and experimental techniques. *Am J Roentgenol*, 157(6):1229-37, 1991.

18. Fedlin ED, Hirsch C: Factors affecting the determination of the physical properties of femoral cortical bone. *Acta Orthop Scand*, 37:29-48, 1966.

19. Fidler M: Incidence of fracture through metastases in long bones. *Acta Orthop Scand*, 52(6):623-7, 1981.

20. Fung YC: Bone and cartilage, in *Biomechanics. Mechanical properties of living tissues*, Springer-Verlag: New York, p. 500-36, 1993.

21. Habermann ET, Sachs R, Stern RE, Hirsh DM, Anderson WJ: The pathology and treatment of metastatic disease of the femur. *Clin Orthop*, :70-82, 1982.

22. Hardman PD, Robb JE, Kerr GR, Rodger A, MacFarlane A: The value of internal fixation and radiotherapy in the management of upper and lower limb bone metastases. *Clin Oncol (R Coll Radiol)*, 4(4):244-8, 1992.

23. Harrington KD: New trends in the management of lower extremity metastases. *Clin Orthop*, 169:53-61, 1982.

24. Harrington KD: *Orthopaedic management of metastatic bone disease.* Mosby: St. Louis, p. 393, 1988.

25. Hayes WC, Piazza SJ, Zysset PK: Biomechanics of fracture risk prediction of the hip and spine by quantitative computed tomography. *Radiol Clin North Am*, 29(1):1-18, 1991.

26. Hipp JA, Cheal EJ, Hayes WC: Biomechanics of fractures, in *Skeletal trauma: fractures, dislocations, ligamentous injuries*, Browner BD, Jupiter JB, Levine AM, Trafton PG, Editor, W. B. Saunders Company: Philadelphia, p. 95-125, 1992.

27. Hipp JA, Edgerton BC, An KN, Hayes WC: Structural consequences of transcortical holes in long bones loaded in torsion. *J Biomech*, 23(12):1261-8, 1990.

28. Hipp JA, Katz G, Hayes WC: Local demineralization as a model for bone strength reductions in lytic transcortical metastatic lesions. *Invest Rad*, 26:934-38, 1991.

29. Hipp JA, McBroom RJ, Cheal EJ, Hayes WC: Structural consequences of endosteal metastatic lesions in long bones. *J Orthop Res*, 7(6):828-37, 1989.

30. Keaveny TM, Hayes WC: Mechanical properties of cortical and trabecular bone, in *Bone*, Hall BK, Editor, CRC Press: Boca Raton, p. 285-344, 1993.

31. Keene JS, Sellinger DS, McBeath AA, Engber WD: Metastatic breast cancer in the femur. A search for the lesion at risk of fracture. *Clin Orthop*, 203:282-8, 1986.

32. Keller TS: Predicting the compressive mechanical behavior of bone. *J Biomech*, 27(9):1159-1168, 1994.

33. Keller TS, Mao Z, Spengler DM: Young's modulus, bending strength, and tissue physical properties of human compact bone. *J Orthop Res*, 8(4):592-603, 1990.

34. Keyak JH, Fourkas MG, Meagher JM, Skinner HB: Validation of an automated method of three-dimensional finite element modelling of bone. *J Biomed Eng*, 15(6):505-9, 1993.

35. Keyak JH, Meagher JM, Skinner HB, Mote CJ: Automated three-dimensional finite element modelling of bone: a new method. *J Biomed Eng*, 12(5):389-97, 1990.

36. Keyak JH, Skinner HB: Three-dimensional finite element modelling of bone: effects of element size. *J Biomed Eng*, 14(6):483-9, 1992.

37. Kuo RF, Chao EY, Rim K, Park JB: The effect of defect size on the stress concentration and fracture characteristics for a tubular torsional model with a transverse hole. *J Biomech*, 24(2):147-55, 1991.

38. Leggon RE, Lindsey RW, Panjabi MM: Strength reduction and the effects of treatment of long bones with diaphyseal defects involving 50% of the cortex. *J Orthop Res*, 6(4):540-6, 1988.

39. Les CM, Keyak JH, Stover SM, Taylor KT, Kaneps AJ: The estimation of material properties in the equine metacarpus using quantitative computed tomography. *J Orthop Res*, 12:822-833, 1994.

40. Lotz JC, Cheal EJ, Hayes WC: Fracture prediction for the proximal femur using finite element models: Part I--Linear analysis. *J Biomech Eng*, 113(4):353-60, 1991.

41. Lotz JC, Cheal EJ, Hayes WC: Fracture prediction for the proximal femur using finite element models: Part II--Nonlinear analysis. *J Biomech Eng*, 113(4):361-5, 1991.

42. Lotz JC, Gerhart TN, Hayes WC: Mechanical properties of metaphyseal bone in the proximal femur. *J Biomech*, 24(5):317-29, 1991.

43. Lotz JC, Hayes WC: The use of quantitative computed tomography to estimate risk of fracture of the hip from falls. *J Bone Joint Surg [Am]*, 72(5):689-700, 1990.

44. Martin RB: Age and strength of bone as a structural material. *Calcif Tissue Int*, 53(Suppl 1):S34-S40, 1993.

45. Martin RB, Burr DB: *Structure, function, and adaptation of compact bone.* Raven Press: New York, p. 275, 1989.

46. McBroom RJ, Cheal EJ, Hayes WC: Strength reductions from metastatic cortical defects in long bones. *J Orthop Res*, 6(3):369-78, 1988.

47. McCalden RW, McGeough JA, Barker MB, Court-Brown CM: Age-related changes in the tensile properties of cortical bone. The relative importance of changes in porosity, mineralization, and microstructure. *J Bone Joint Surg*, 75A(8):1193-205, 1993.

48. Mizrahi J, Silva MJ, Hayes WC: Finite element stress analysis of simulated metastatic lesions in the lumbar vertebral body. *J Biomed Eng*, 14(6):467-75, 1992.

49. Murray JA, Parrish FF: Surgical management of secondary neoplastic fractures about the hip. *Orthop Clin North Am*, 5(4):887-901, 1974.

50. Myers MH, Ries LA: Cancer patient survival rates: SEER program results for 10 years of follow-up. *Ca Cancer J Clin*, 39(1):21-32, 1989.

51. Nordin M, Frankel VH: Biomechanics of bone, in *Basic biomechanics of the musculoskeletal system*, Leas & Febiger: Philidelphia, PA, p. 3-29, 1989.

52. Ortiz Gómez JA: The incidence of vertebral body metastases. *International Orthopaedics (SICOT)*, 19:309-11, 1995.

53. Peterson RE: *Stress concentration design factors*. Wiley: New York, p. 155, 1953.

54. Reilly DT, Burstein AH: The elastic and ultimate properties of compact bone tissue. *J Biomech*, 8(6):393-405, 1975.

55. Ricos V, Pedersen DR, Brown TD, Ashman RB, Rubin CT, Brand RA: Effects of anisotropy and material axis registration on computed stress and strain distributions in the turkey ulna. *J. Biomech*, 29(2):261-67, 1996.

56. Ross MH, Reith EJ, Romrell LJ: Bone, in *Histology. A text and atlas*, Williams & Wilkins: Baltimore, p. 141-64, 1989.

57. Rubens RD, Fogelman I: *Bone metastases: diagnosis and treatment*. Springer-Verlag: London, p. 247, 1991.

58. Schaffler MB, Burr DB: Stiffness of compact bone: effects of porosity and density. *J Biomech*, 21(1):13-6, 1988.

59. Schurman DJ, Amstutz HC: Orthopedic management of patients with metastatic carcinoma of the breast. *Surg Gynecol Obstet*, 137(5):831-6, 1973.

60. Seitz P, Ruegsegger: Fast contour detection algorithm for high precision quantitative CT. *IEEE Trans on Med Imag*, MI-2(3):136-141, 1983.

61. Snyder SM, Schneider E: Estimation of mechanical properties of cortical bone by computed tomography. *J Orthop Res*, 9(3):422-31, 1991.

62. Stephens T: A mixed bag of cancer trends. *J NIH Res*, 3:71-2, 1991.

63. Stromsoe K, Hoiseth A, Alho A, Kok WL: Bending strength of the femur in relation to non-invasive bone mineral assessment. *J. Biomech*, 28(7):857-861, 1995.

64. Sumner DR, Olson CL, Freeman PM, Lobick JJ, Andriacchi TP: Computed tomographic measurement of cortical bone geometry. *J Biomech*, 22(6-7):649-53, 1989.

65. Tsai S, Wu E: A general theory for strength of anisotropic materials. *J Composite Mater*, 5:58-80, 1971.

66. Van Buskirk WC, Cowin SC, Ward RN: Ultrasonic measurement of orthotropic elastic constants of bovine femoral bone. *J Biomech Eng*, 103(2):67-72, 1981.

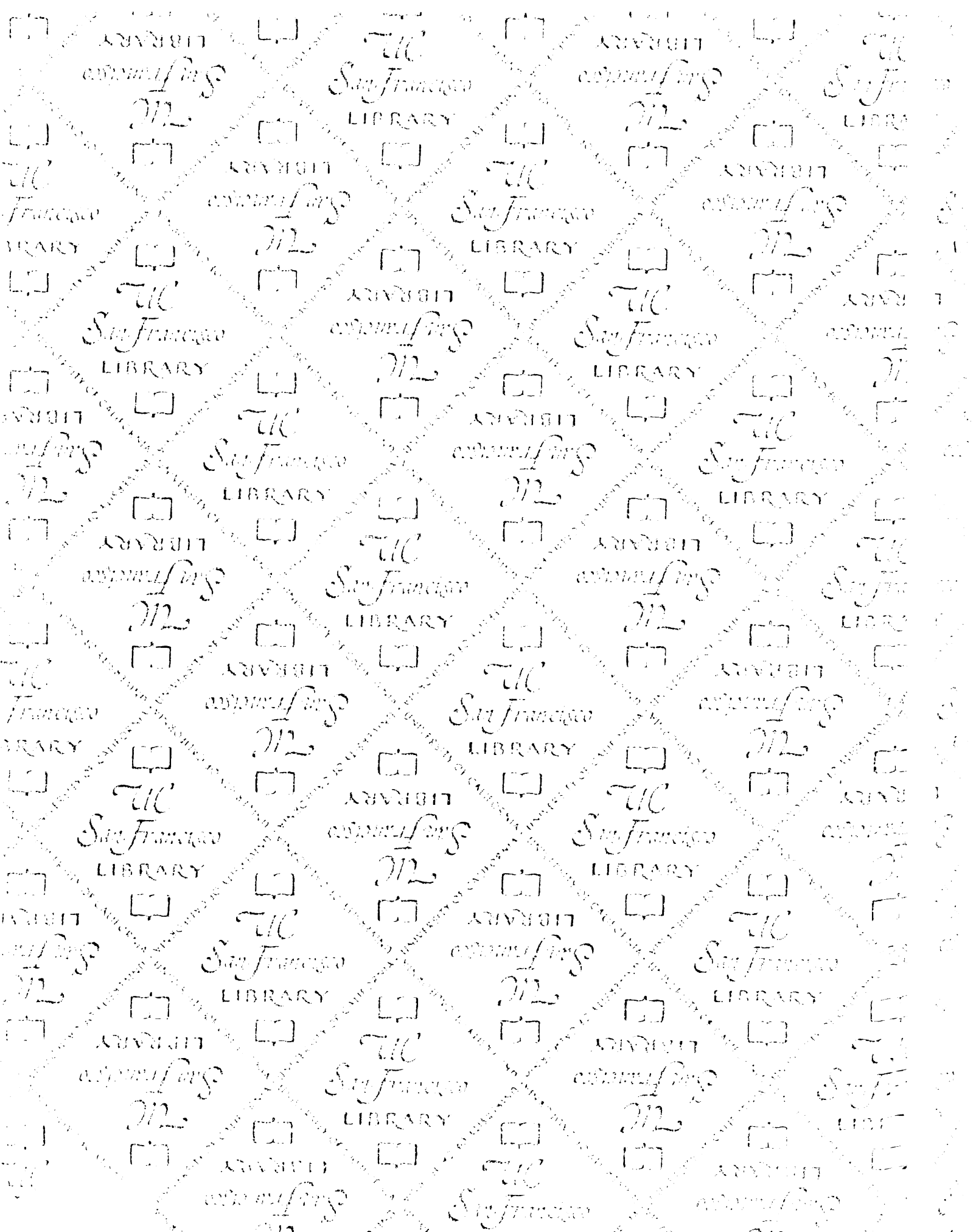
The San Francisco LIBRARY

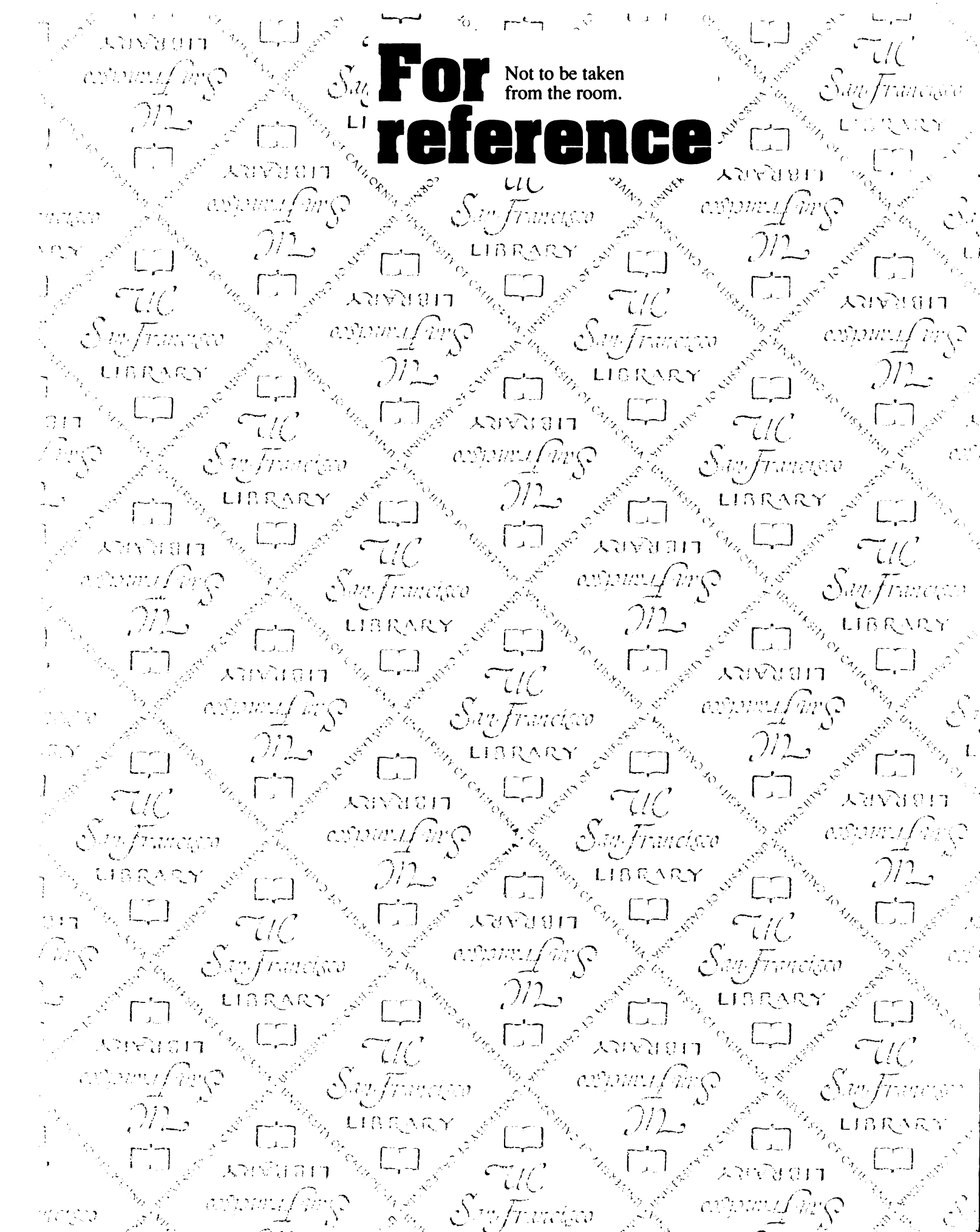
For reference
Not to be taken from the room.
UC San Francisco LIBRARY